Effect of combined sodium arsenite and cadmium chloride treatment on heat shock protein gene expression in *Xenopus laevis* A6 kidney epithelial cells

by

Imran Khamis

A thesis
presented to the University of Waterloo
in fulfillment of the
thesis requirement for the degree of
Master of Science
in
Biology

Waterloo, Ontario, Canada, 2013

Author's Declaration

I hereby declare that I am the sole author of this thesis. This is a true copy of the thesis, including any required final revisions, as accepted by my examiners.

I understand that my thesis may be made electronically available to the public.

Abstract

Sodium arsenite and cadmium chloride are two widespread environmental toxicants which have deleterious effects on living organisms. At the cellular level, sodium arsenite and cadmium chloride cause oxidative stress, dysregulation of gene expression, apoptosis, and the unfolding of protein. Furthermore, both chemical stressors individually have the ability to induce heat shock protein (HSP) accumulation. HSPs are molecular chaperones that aid in protein folding, translocation and in preventing stress-induced protein aggregation. Previously, our laboratory demonstrated that treatment of A6 kidney epithelial cells of the frog *Xenopus laevis*, with either cadmium chloride or sodium arsenite plus a concurrent mild heat shock resulted in an enhanced accumulation of HSPs that was greater than found with the sum of the individual stressors. To the best of our knowledge, no information is available to date on the effect that these two chemical stressors have in combination on HSP accumulation in aquatic organisms. The present study examined the effect of simultaneous sodium arsenite and cadmium chloride treatment on the pattern of HSP30 and HSP70 accumulation in *Xenopus* A6 cells. Immunoblot analysis revealed that the relative levels of HSP30 and HSP70 accumulation in A6 cells treated concurrently with sodium arsenite and cadmium chloride for 12 h were significantly higher than the sum of HSP30 or HSP70 accumulation from cells subjected to the treatments individually. For instance, the combined 10 µM sodium arsenite plus 100 µM cadmium chloride treatment resulted in a 3.5 fold increase in HSP30 accumulation and a 2.5 fold increase in HSP70 accumulation compared to the sum of the stressors individually. This finding suggested a synergistic action between the two stressors. Pretreatment of cells with KNK437, an HSF1 inhibitor, inhibited the combined sodium arsenite- and cadmium chloride-induced accumulation of HSP30 and HSP70 suggesting that this accumulation of HSPs may be regulated, at least in

part, at the level of transcription. Immunocytochemical analysis employing the use of laser scanning confocal microscopy (LSCM) revealed that simultaneous treatment of cells with the two stressors induced HSP30 accumulation primarily in the cytoplasm in a punctate pattern with some dysregulation of F-actin structure. Increased ubiquitinated protein accumulation was observed with combined 10 µM sodium arsenite and 10, 50 or 100 µM cadmium chloride treatment compared to individual stressors suggesting an impairment of the ubiquitin-proteasome degradation system. Finally, while incubation of A6 cells with 1 µM sodium arsenite plus 10 µM cadmium chloride did not induce a detectable accumulation of HSPs, the addition of a 30 °C mild heat shock resulted in a strong accumulation of HSP30 and HSP70. This study has demonstrated that concurrent sodium arsenite and cadmium chloride treatment can enhance HSP accumulation. Since HSP accumulation is triggered by proteotoxic stress, these findings are relevant given the fact that aquatic amphibians in their natural habitat may be exposed to multiple chemical stressors simultaneously.

Acknowledgements

What a memorable few years! Throughout my time in the Heikkila lab, I have gained a vast amount of knowledge and valuable experience which I am truly grateful for. First off, I would like to thank my supervisor, Dr. John J. Heikkila, for giving me this opportunity. Your patience, advice and guidance in these last two years has been invaluable. To my committee members, Dr. Bernard Duncker and Dr. Brian Dixon, thank you for reading my work and providing helpful feedback. Next, I would like to thank my lab mates past and present who provided me with some great memories: Jara, AJ, Charles, Ena and Saad. A special thanks also goes out to Saad for training me, putting up with my constant questions, and helping me out whenever I needed it. Most importantly, I would like to thank my family for always being there for me - giving me the utmost love and support.

Table of Contents

Author's Declaration ii

Abstract iii

Acknowledgements v

Table of Contents vi

List of Figures viii

List of Abbreviations x

1. Introduction 1

1.1 Heat shock proteins 1

1.2 Heat shock response 2

1.3 *Hsp* gene regulation 2

1.4 Small heat shock proteins 6

1.5 Heat shock protein 70 8

1.6 Sodium arsenite 9

1.7 Cadmium chloride 10

1.8 Protein degradation 11

1.9 Ubiquitin-proteasome system 11

1.9.1 Protein ubiquitination 14

1.9.2 The proteasome 14

1.9.2 Proteasomal inhibition 15

1.10 *Xenopus laevis* as a model organism 15

1.11 Heat shock response in *Xenopus laevis* 16

1.11.1 *Xenopus* HSP30 17

1.11.2 *Xenopus* HSP70 19

1.11.3 Effect of sodium arsenite and cadmium chloride on HSP accumulation in *Xenopus* 19

1.12 Objectives 20

2. Materials and Methods 22

2.1 Maintanence and treatment of *Xenopus laevis* cells 22

2.2 Protein isolation and quantification 23

2.3 SDS-Polyacrylamide gel electrophoresis 24

2.3.1 Immunoblotting 25

2.4 Densitometry and statistical analysis 26

2.5 Immunocytochemistry and laser scanning confocal microscopy 26

3. Results 28

3.1 Comparison of stress-induced HSP30 accumulation in A6 cells and XTC-2 cells 28

3.2 Effect of various heavy metals on HSP30 accumulation in A6 cells 28

3.3 Effect of simultaneous sodium arsenite and cadmium chloride treatment on HSP30 and HSP70 accumulation in A6 cells 37

3.4 Effect of KNK437 on HSP30 and HSP70 accumulation in cells exposed simultaneously to sodium arsenite and cadmium chloride treatment 53

3.5 HSP30 localization in cells treated concurrently with sodium arsenite and cadmium chloride 56

3.6 Effect of simultaneous sodium arsenite and cadmium chloride treatment on ubiquitinated protein levels 63

3.7 Effect of a concurrent mild heat shock plus low concentrations of sodium arsenite and cadmium chloride on HSP30, HSP70 and ubiquitinated protein accumulation 63

4. Discussion 71

References 79

List of Figures

Figure 1. The heat shock response 4

Figure 2. Protein degradation by the UPS. 12

Figure 3. Comparison of heat shock-induced HSP30 accumulation in A6 and XTC-2 cells. 29

Figure 4. Comparison of the effect of sodium arsenite on HSP30 accumulation in A6 and XTC-2 cells. 31

Figure 5. Effect of zinc sulfate on HSP accumulation and cell morphology in A6 cells 33

Figure 6. Effect of lead nitrate on HSP accumulation and cell morphology in A6 cells 35

Figure 7. Effect of copper sulfate on HSP accumulation and cell morphology in A6 cells 38

Figure 8. Enhanced accumulation of HSP30 and HSP70 after a 12 h concurrent exposure to 10 µM sodium arsenite plus 10, 50 or 100 µM cadmium chloride 40

Figure 9. Effect of a 16 h concurrent sodium arsenite and cadmium chloride treatment on HSP30 and HSP70 accumulation 43

Figure 10. Effect of sodium arsenite and/or cadmium chloride on A6 cell morphology. 45

Figure 11. Time course of HSP30 and HSP70 accumulation in A6 cells treated simultaneously with low concentrations of sodium arsenite and cadmium chloride. 47

Figure 12. Extended time course of HSP30 and HSP70 accumulation in A6 cells treated simultaneously with low concentrations of sodium arsenite and cadmium chloride 49

Figure 13. Effect of either 2.5 or 5 µM sodium arsenite plus 50 µM cadmium chloride on HSP30 and HSP70 accumulation. 51

Figure 14. Effect of KNK437 on the accumulation of HSP30 and HSP70 in A6 cells treated concurrently with sodium arsenite and cadmium chloride. 54

Figure 15. Detection of HSP30 accumulation in A6 cells exposed to 10 μM sodium arsenite and/or 10 μM cadmium chloride. 57
Figure 16. Detection of HSP30 accumulation in A6 cells exposed to 10 μM sodium arsenite and/or 50 μM cadmium chloride. 59
Figure 17. Detection of HSP30 accumulation in A6 cells exposed to 10 μM sodium arsenite and/or 100 μM cadmium chloride. 61
Figure 18. Effect of combined sodium arsenite and cadmium chloride treatment on ubiquitinated protein accumulation in A6 cells. 64
Figure 19. Accumulation of HSP30 and HSP70 in A6 cells treated simultaneously with relatively low concentrations of sodium arsenite, cadmium chloride plus a mild heat shock. 66
Figure 20. Effect of combined low concentrations of sodium arsenite and cadmium chloride plus mild heat shock treatment on ubiquitinated protein accumulation in A6 cells. 68
Figure 21. Proposed mechanism of synergistic action of low concentrations of sodium arsenite plus cadmium chloride. 74

List of abbreviations

ANOVA	analysis of variance
APS	ammonium persulfate
As	sodium arsenite
BCA	bicinchoninic acid
BiP	immunoglobulin-binding protein
BSA	bovine serum albumin
C	control
Cd	cadmium chloride
$CuSO_4$	copper sulfate
DAPI	4,6-diamidino-2-phenylindole
EDTA	ethylene-diamine-tetraacetic acid
ER	endoplasmic reticulum
GADD	growth arrest and DNA damage
HBSS	Hank's balanced salt solution
HDI	histone deacetylase inhibitor
HEPES	4-(2-hydroxyethyl)-1-piperazineethanesulfonic acid
HSC	heat shock cognate
HSE	heat shock element
HSF	heat shock factor
HSP	heat shock protein
hsp	heat shock protein gene or mRNA
HSR	heat shock response
KNK437	N-formyl-3, 4-methylenedioxy-benzylidene-γ-butyrolactam
L-15	Leibovitz-15
LSCM	laser scanning confocal microscopy
MBT	mid-blastula transition
MG132	carbobenzoxy-L-leucyl-L-leucyl-L-leucinal
$Pb(NO_3)_2$	lead nitrate
PBS	phosphate buffered saline
PMS2	postmeiotic segregation increased 2
SDS-PAGE	sodium dodecyl sulfate-polyacrylamide gel electrophoresis
SHSP	small heat shock protein
TBS-T	tris buffered saline solution – Tween20
TEMED	tetra-methyl-ethylene-diamine
TRITC	rhodamine-tetramethylrhodamine-5-isothiocyanate phalloidin
UPS	ubiquitin-proteasome system
XTC-2	*Xenopus* tissue culture
$ZnSO_4$	zinc sulfate

1. Introduction

Organisms in their natural environment may be exposed to various stressful stimuli, which can affect cellular protein function and stability (Morimoto, 1998; Balch et al., 2008). Upon stressful conditions, the unfolding or misfolding of proteins can result in aggregation, which can lead to harmful cytotoxic effects and potential disease states (Morimoto, 2008). Key molecular mechanisms have evolved to counteract these stresses including the accumulation of stress inducible proteins known as the heat shock proteins (HSPs).

1.1 Heat Shock Proteins

In 1962, Ferruccio Ritossa discovered in *Drosophila* that a temporary increase in temperature resulted in a change in the puffing pattern of salivary gland polytene chromosomes, which ultimately led to the discovery of HSPs, the cloning of their genes and analysis of their stress-inducible regulation (Ritossa, 1962; Morimoto, 1998; 2008). HSPs are an extensive group of molecular chaperones that assist in protein folding and synthesis under normal conditions (Morimoto, 2008). In general, HSPs are highly conserved and have been found in essentially all organisms from bacteria to humans (Kregel, 2002). Stress-inducible HSPs aid in preventing stress-induced aggregation of unfolded proteins and are involved in their refolding once the stress has been alleviated or in their degradation if the damage is too severe (Morimoto, 1998; 2008). There are at least six major families of HSPs that have been classified primarily by size: HSP100, HSP90, HSP70, HSP60, HSP40 and the small heat shock proteins (sHSPs) (Katschinski, 2004). Some of the HSPs are stress inducible, while others are constitutively expressed.

1.2 Heat Shock Response

The prokaryotic and eukaryotic heat shock response (HSR) is a molecular mechanism, which involves the upregulation of HSP accumulation that is initiated to counteract and protect cells against stress-induced proteotoxic stress (Morimoto, 2008). Proteotoxic stress in the cell is characterized by unfolded or misfolded protein, formation of protein aggregates and loss of protein function. Various stressors that were reported to induce the HSR include elevated temperatures, proteasomal inhibitors, chemical stressors (including sodium arsenite and cadmium chloride) or various disease states (Morimoto, 2008). Certain neurodegenerative diseases such as amyotrophic lateral sclerosis, Alzheimer's, Huntington's and Parkinson's, which can lead to a build-up of unfolded protein aggregates, are associated with the synthesis or mutation of selected HSPs. Current research is directed toward the use of HSPs or *hsp* gene expression as a therapeutic approach to decrease the amount of toxic aggregates in these diseased states. Given the therapeutic potential of HSPs, a large amount of research has been directed toward fully understanding the regulation of the HSR and HSP function.

1.3 *Hsp* Gene Regulation

Although heat shock-induced *hsp* gene expression is regulated primarily at the transcriptional level, regulation at the level of mRNA stability and translation have also been documented (Heikkila et al., 1997; Kim and Jang, 2002). Constitutive or stress-inducible transcription of *hsp* genes involves the binding of a transcription factor, heat shock factor (HSF), to the enhancer, heat shock element (HSE), in the promoter region of the gene (Voellmy, 2004). At least 4 different HSFs with distinct functions have been identified to date (Morimoto and Santoro, 1998; Voellmy, 2004). Mammals possess at least 3, namely, HSF1, HSF2 and HSF4, while HSF3 is avian specific (Voellmy, 2004; Yamamoto et al., 2009). HSF1, which is the

vertebrate homolog of yeast HSF, can be activated by various stressors (Morimoto, 1998; Voellmy, 2004). HSF2 was reported to be activated during certain stages of animal development. HSF3 was found to be involved in stress-induced *hsp* gene expression in birds (Rallu et al., 1997; Voellmy, 2004). HSF4 is functionally distinct and exhibits tissue-specific expression, with preferential expression observed in the human heart, brain, skeletal muscle and pancreas (Nakai et al., 1996).

As described above, HSF1 is the stress-responsive member of the HSF family and is responsible for the activation of the HSR in higher organisms (Voellmy, 2004). It is thought that an accumulation of unfolded or misfolded proteins leads to the activation of HSF1 (Fig. 1; Georgopoulos and Welch, 1993; Krebs and Feder 1997; Morimoto 1998). The structure of HSF1 is highly conserved, and consists of 100 amino acids in a helix-turn-helix DNA binding motif, as well as a transcriptional transactivation domain, a carboxy-terminal hydrophobic region and an oligomerization domain essential for trimer formation. HSF1 occurs as an inactive cytosolic monomer bound to HSP90 in non-stressed cells (Morimoto, 1998; 2008; Heikkila, 2010). Upon stressful stimuli such as heat shock or sodium arsenite treatment, HSP90 dissociates from HSF1, as it is recruited to other areas of the cell to counteract the stress and carry out its duties as a molecular chaperone; to bind to and prevent aggregation of unfolded protein (Morimoto, 1998; 2008). This dissociation of HSP90 from HSF1 causes HSF1 monomers to trimerize (Voellmy, 2004). The trimerized HSF1 is then hyperphosphorylated at serine and threonine residues, which is followed by its translocation to the nucleus. HSF1 then binds to the HSE, located in the 5' promoter of *hsp* genes to facilitate transcription by RNA polymerase II, resulting in the

Figure 1. The heat shock response. (1) Environmental stress or disease states can cause native proteins to unfold. (2) Under normal conditions, HSP90 is bound to heat shock factor 1 (HSF1) in the cell and upon stress, is recruited to prevent aggregation of unfolded proteins. (3) This allows HSF1 monomers to trimerize, become hyperphosphorylated and translocate to the nucleus. (4) The HSF1 trimer binds to the heat shock element (HSE) located in the 5' promoter of *hsp* genes initiating transcription by RNA polymerase II. (5) Stress-induced HSPs accumulate and are recruited to the unfolded protein to prevent its aggregation and to maintain it in a folding competent state. (6) The drug KNK437 can specifically inhibit the activation of HSF1.

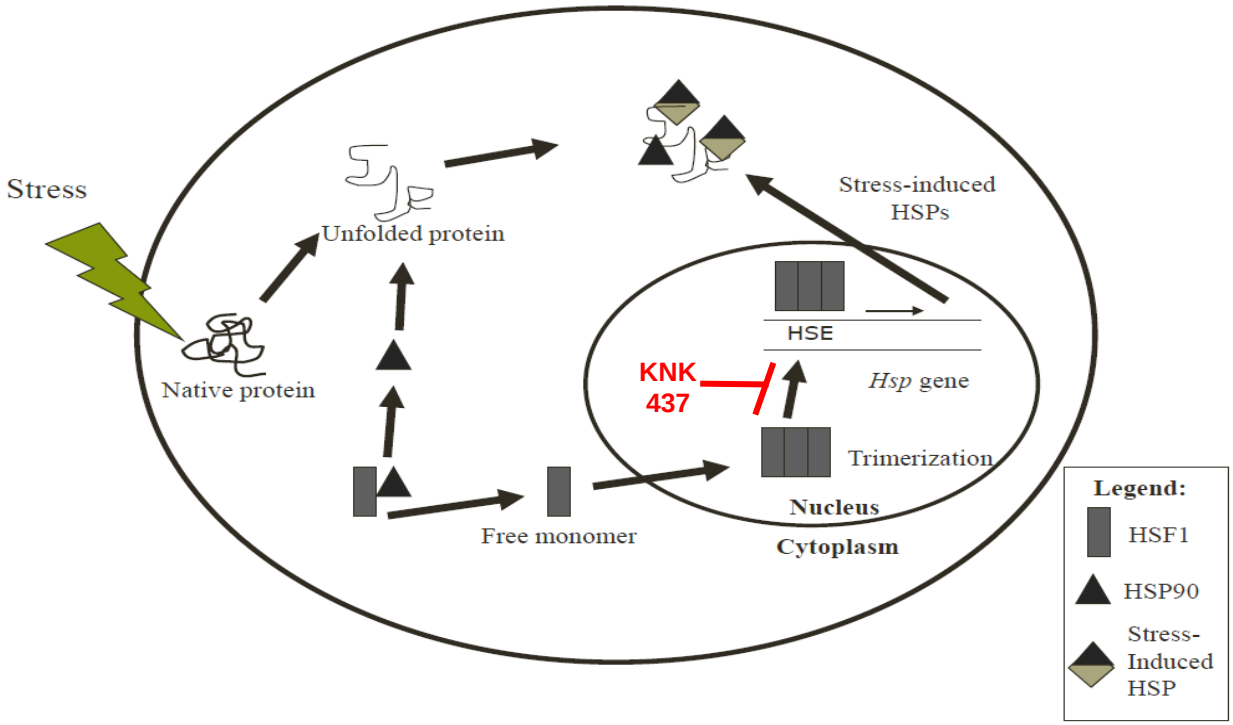
Stress
Native protein
Unfolded protein
Free monomer
Stress-induced HSPs
HSE
KNK 437
Hsp gene
Trimerization
Nucleus
Cytoplasm
Legend:
HSF1
HSP90
Stress-Induced HSP

accumulation of HSPs to bind to unfolded protein to counteract proteotoxic stress (Voellmy, 2004; Heikkila, 2010). The N-terminal DNA binding domain is the site at which HSF1 interacts with the HSE, and there is at least one HSE present within all promoters of stress-inducible *hsp* genes. Previous studies have also employed a chemical known as KNK437 (N-formyl-3,4-methylenedioxy-benzylidene-γ-butyrolactam), a benzylidene lactam compound, which was found inhibit the transcription of *hsp* genes by repressing the interaction of HSF1 with HSE as shown in gel shift assays (Ohnishi et al., 2004). The inhibitory action of KNK437 on HSP accumulation in mammalian cells was reported to be similar to cells treated with siRNA directed against HSF1 mRNA (Song et al., 2010; Liu et al., 2012).

1.4 Small Heat Shock Proteins

SHSPs range in size from 12 to 43 kDa and are highly divergent except for an α-crystallin domain which is 80-100 amino acids long (MacRae, 2000; Van Montfort et al., 2001). The lack of conservation among sHSPs and the evolutionary divergence compared to other HSP families results in structural homology being quite low between family members (MacRae, 2000; Van Montfort et al., 2001). SHSPs appear to have roles in actin capping and decapping, cellular differentiation, prevention of apoptosis and the acquisition of thermotolerance (Arrigo, 1998; MacRae, 2000; Van Montfort et al., 2001; Heikkila, 2004). SHSPs contain at least 3 functional domains including the C-terminal α-crystallin domain, an amino-terminal region as well as a carboxy-terminal extension. The α-crystallin domain is vital for dimerization, a functional characteristic seen with these heat shock proteins (Buchner et al., 1998; MacRae, 2000; Sun and MacRae, 2005). The N-terminal region aids in oligomeric formation, while the C-terminal end plays a role in protein stabilization as well as chaperone activity (Lambert, 1999; Ganea, 2001; MacRae, 2000; Fernando and Heikkila, 2000). Carboxy-terminal extensions of sHSPs are

variable in sequence and length but normally contain polar amino acids, which are essential for their solubility.

The accumulation of unfolded or misfolded protein induced by various stressors such as heat shock, sodium arsenite or cadmium chloride triggers the activation of the HSR and expression of *shsp* genes. As mentioned previously, it is essential to inhibit the build-up of aggregated proteins as this can lead to cellular toxicity. Stress-induced sHSPs form multimeric complexes that bind to unfolded target proteins, maintain them in a soluble state and prevent their aggregation so that they can be refolded by other ATP-dependent chaperones such as HSP70, once normal conditions have returned. The multimeric complex formation of sHSPs (conserved in a number of organisms including yeast, mammals and amphibians) is essential for the molecular chaperone function of sHSPs (Ohan et al., 1998; MacRae, 2000; Heikkila, 2003; Sun and MacRae, 2005). SHSPs are quite effective as chaperones, as one oligomeric sHSP complex was found to have the capacity to bind a large number of non-native proteins (Haslbeck, 2002). After the removal of stress, sHSP oligomers become phosphorylated, resulting in a change in the secondary structure and a breakdown of the multimeric complex, therefore limiting their role as molecular chaperones (Lambert et al., 1999; Fernando et al., 2003). However, some phosphorylated sHSPs have been shown to interact with F-actin filaments or monomeric F-actin to influence actin polymerization and/or depolymerization (Sun and MacRae, 2005).

Intracellular localization of sHSPs varies based on the type of sHSP, the physiological state of the cells and intensity of the stressor, as observed with *Drosophila*, *Xenopus* and mouse (Beaulieu et al., 1989; Adhikari et al., 2004; Gellalchew and Heikkila, 2005; Heikkila, 2010). With a given type of sHSP, amino acid sequence variation is conserved among family members in a species but is not as well conserved across species. (Arrigo and Landry, 1994; Stromer et al.,

2003). Also, multiple members of sHSP families have been documented in bacteria, plants, insects, nematodes, crustaceans, amphibians and mammals (Allen et al., 1992; Wotton et al., 1996; Boston et al., 1996; Waters et al., 1996; Linder et al., 1996; Michaud et al., 1997; Liang et al., 1997; Ohan et al., 1998a; MacRae, 2000; Sun and MacRae, 2005; Heikkila, 2010).

1.5 Heat Shock Protein 70

The 70-kDa heat shock protein family is highly conserved in different species, and contains molecular chaperones that are responsible for regulating protein folding under normal and stressful conditions (Daugaard et al., 2007). HSP70 is present in all organisms and consists of multiple family members (Katschinski, 2004). In eukaryotes, the HSP70 family consists of the cytoplasmic stress-inducible HSP70, constitutively expressed heat shock cognate 70 (HSC70), mitochondrial HSP70 and the resident endoplasmic reticulum HSP70 family member, immunoglobulin binding protein, also referred to as glucose regulated protein 78 (BiP). The HSP70 molecule is composed of a highly conserved ATP-binding domain at the N-terminal end, and a C-terminal peptide binding domain containing a motif allowing for HSP70 to bind co-chaperones as well as other HSPs (Beere et al., 2000; Daugaard et al., 2007). The HSP70s, in an ATP-dependent manner, help to prevent aggregation as well as playing a major role in the refolding of unfolded proteins. Also, HSP70 was reported to play a role in preventing cell death, by interacting with certain factors that inhibit caspase-dependent apoptosis (Beere et al., 2000; Daugaard et al., 2007). Under non-stressful conditions, HSP70 was suggested to play a role in translocation of proteins. For instance, HSP70s have roles in the import of cytoplasmic proteins into the mitochondria or endoplasmic reticulum (ER). This was observed with BiP; an HSP70 family member that helps to transport newly synthesized proteins into the ER lumen and is subsequently involved with its folding (Zimmerman et al. 2006). Cellular stress initiates

translocation of HSC70 and HSP70 to the nucleus, which is facilitated by the presence of a nuclear localization signal (Ali et al., 1996a). Also, cytosolic HSP70 has the ability to interact with growing polypeptide chains as they emerge from the ribosome and to prevent their aggregation (Beckmann et al., 1990; Georgopoulos and Welch, 1993).

1.6 Sodium Arsenite

Sodium arsenite is detrimental to human and animal health (Del Razo et al., 2001). A major source of arsenite exposure in humans occurs with the consumption of contaminated water, which subjects nearly one hundred million people worldwide to an elevated risk of cancer. The presence of arsenite in ground water is the result of minerals being dissolved naturally from weathered rocks and soils (Del Razo et al., 2001). Additionally, environmental arsenite contamination can occur with industrial emissions, which results in an elevated risk of renal, cardiovascular and hepatic cancers (Del Razo et al., 2001). At the cellular level, sodium arsenite can induce cell cycle arrest, as this toxicant causes DNA damage, which is repaired during the S-phase of the cell cycle (Li and Chou, 1992; Del Razo et al., 2001). Arsenite was also observed to induce DNA damage-inducible proteins, GADD45 and GADD143, as well as the DNA mismatch repair protein PMS2 (Liu et al., 2001). Arsenite was found to cause a marked inhibition in the synthesis of cytoskeletal proteins and given the high affinity of arsenite for sulfhydryl groups, researchers have also observed a lack of cross-linking of adjacent actin microfilaments leading to cytoskeletal injury (Li and Chou, 1992). Activation of apoptotic pathways by arsenite was indicated by an enhanced level of caspase-3 activity, leading to the hydrolysis of protein targets (Liu et al., 2001). Glucose homeostasis can also be affected by presence of arsenite since it reduced the transcription of two main hepatocyte nuclear factors (HNF1-α and HNF4-α) (Pastoret et al., 2012). Since these transcription factors are required for

normal functioning of the liver, there is an increased risk of diabetes in humans exposed to arsenite. The effect of sodium arsenite on the ubiquitin-proteasome system (UPS) has been studied primarily in mammalian systems. It was reported that arsenite inhibited proteasomal activity as indicated by an increase in the relative levels of ubiquitinated protein and a decrease in chymotrypsin-like activity (Tsou et al., 2005; Medina-Diaz et al., 2009; Kirkpatrick, 2003). Finally, arsenite was shown in numerous studies to induce the accumulation of HSPs by means of HSF1 activation triggered by the intracellular elevation of unfolded or damaged protein (Voellmy, 2004).

1.7 Cadmium Chloride

Cadmium, a potent human carcinogen, is a heavy metal that accumulates in all major organs, especially the kidney (Bonham et al. 2003; Loumbourdis 2005; Mendez-Armenta and Rios 2007). In humans, cadmium accumulation can be due to anthropogenic sources, the inhalation of tobacco smoke, contaminated food, air pollution or the use of some fertilizers (Waisberg et al. 2003). Cadmium, being a category one human carcinogen, was shown to cause cancers of the lung, prostate and pancreas (Waisberg et al., 2003). In aquatic organisms, cadmium enters dermally through the skin and gills, and exposure results in the formation of denatured or damaged proteins as well as developmental abnormalities (Pederson and Bjerregaard, 2000; Fort et al., 2001; Waisberg et al., 2003). The presence of cadmium has many negative effects at the cellular and physiological level (Waisberg et al., 2003). Cadmium can induce the production of reactive oxygen species (ROS). Furthermore, cadmium-induced increase in transcriptional activation of immediate early response genes can result in tumourigenesis. Cadmium was also found to disrupt E-cadherin mediated cell adhesion, inhibit DNA repair and cellular calcium pathways and proteasomal activity (Joseph et al. 2001;

Waisberg et al., 2003; Yu et al., 2008). Also, cadmium-induced activation of protein kinases resulted in an increased amount of protein phosphorylation and expression of proto-oncogene transcription factors, causing abnormal levels of cell growth and proliferation. Finally, cadmium treatment of cells was reported to induce the accumulation of HSPs and metallothioneins, which have important roles in cellular defensive mechanisms (Waisberg et al., 2003).

1.8 Protein Degradation

There are two main protein degradation pathways that are utilized by eukaryotes. The lysosomal degradation pathway, which hydrolyses extracellular protein, plays a relatively minor role in cellular protein degradation (Lee and Goldberg, 1998). The ubiquitin-proteasome pathway, on the other hand, has a major role in degradation, through hydrolysis of cellular protein in an ATP-dependent manner (Lee and Goldberg, 1998).

1.9 Ubiquitin-Proteasome System

The initial discovery of the components of the Ubiquitin-Proteasome System (UPS) began in the early 1980s (Hershko et al., 1980; Ciechanover et al., 1980, Wilkinson et al., 1980; Hough et al., 1987). The UPS, which is present in both the cytoplasm and nucleus, is the major degradation pathway crucial for the removal of damaged cellular proteins. It was determined that 80-90% of cellular proteins are degraded in the proteasome (Lee and Goldberg, 1998a). As shown in Figure 2, the system for the elimination of proteins requires two successive steps: the addition of ubiquitin molecules onto the proteins, which have been targeted for degradation, and the subsequent degradation by the 26S proteasome (Yang et al., 2008).

Figure 2. Process of cellular protein degradation by the UPS. (1) Polypeptides targeted for degradation are tagged with the addition of ubiquitin molecules by the ubiquitinating enzymes in the presence of ATP. (2) Polyubiquitinated proteins are recognized by the 19S regulatory particle of the 26S proteasome. (3) The proteins are then degraded within the 20S core resulting in the generation of small peptides. (4) Some of these peptides are further degraded into amino acids, or transported to the cell surface for antigen presentation (Adapted from Lee and Goldberg, 1998).

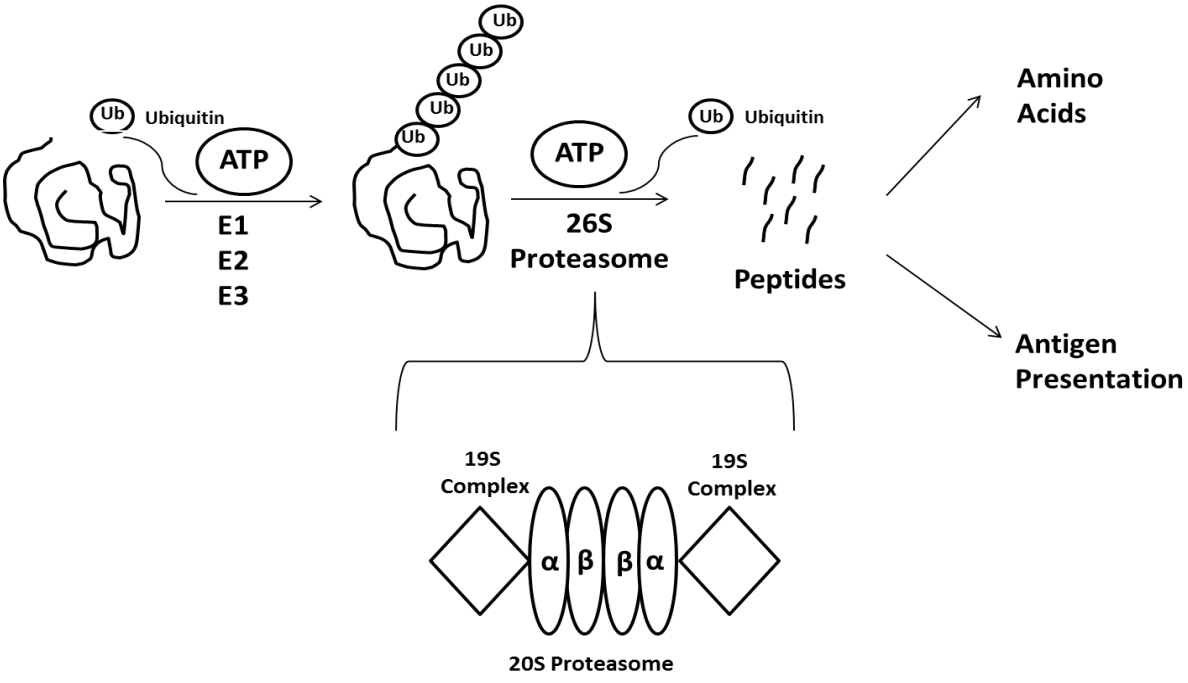
Ub
Ubiquitin
ATP
E1
E2
E3
Ub
Ub
Ub
Ub
Ub
ATP
26S
Proteasome
Ub
Ubiquitin
Peptides
Amino
Acids
Antigen
Presentation
19S
Complex
19S
Complex
α
β
β
α
20S Proteasome

1.9.1 Protein Ubiquitination

Ubiquitin is a small molecular weight protein, which forms an isopeptide bond between a lysine residue on the target protein and the carboxy terminus of ubiquitin (Lee and Goldberg, 1998; Tai and Schuman, 2008). The process of ubiquitination is used to target protein for degradation via the UPS. Ubiquitination involves activating and conjugating enzymes classified as E1, E2, E3 and E4. E1 activates ubiquitination in an ATP-dependent manner through the process of adenylation as well as formation of a thiol-ester bond at the C-terminus end. E2 and E3 (a ubiquitin ligase), help to transfer the ubiquitin molecule to a lysine residue of the protein targeted for degradation. This process occurs repeatedly such that lysine residues are polyubiquitinated with the assistance of E4 (Hershko and Ciechanover, 1998; Koegl et al., 1999). The final step in the ubiquitination process is the delivery of the polyubiquitinated protein to the proteasome.

1.9.2 The Proteasome

The 26S proteasome is comprised of the 20S proteolytic core as well as two 19S regulatory regions. The regulatory region plays a role in recognizing the polyubiquitinated protein targeted for degradation, helps in deubiquitination and unfolds polyubiquitinated proteins which are passed onto the 20S proteolytic core (Bedford et al., 2010; Lee and Goldberg, 1998). The 20S core is comprised of two catalytic β rings surrounded by two non-catalytic α-rings. The α subunits have small openings required for the entrance of polypeptides, whereas β subunits contain proteolytic sites that function together in protein degradation (Lee and Goldberg, 1998). In eukaryotes, the β-rings have catalytic sites with chymotrypsin-like, trypsin-like and caspase-like activity (Lee and Goldberg, 1998). Exopeptidases break down most peptide products into amino acids, while others are transported to the endoplasmic reticulum lumen by a transporter

associated with antigen presentation. These peptides are subsequently displayed on the surface of the cell for antigen presentation after binding to the major histocompatibility complex class 1 molecules (Bogyo et al., 1997; Lee and Goldberg, 1998).

1.9.3 Proteasomal Inhibition

Inhibition of the proteasome leads to a disruption of proteolysis. Severe proteasomal inhibition can result in aggregation of unfolded protein, apoptosis and cell cycle arrest (Yang et al., 2008). The impairment of the UPS has been associated with various disease states including Alzheimer's, Huntington's and Parkinson's disease (Masliah et al., 2000; Ross and Pickart, 2004). In Parkinson's disease, the mechanism by which brain cells are lost arise as a result of abnormal accumulation of the protein α-synuclein, bound to ubiquitin. The α-synuclein-ubiquitin complex cannot be directed to and then degraded in the proteasome. The accumulation of the α-synuclein-ubiquitin complex forms toxic proteinaceous cytoplasmic inclusions referred to as Lewy bodies (Masliah et al., 2000).

1.10 *Xenopus laevis* as a Model Organism

Xenopus laevis, the South African clawed frog, is a popular model organism that has been used extensively in research over the last century to study cell and developmental biology. Thus, a large amount of information is available about its biology at both the cellular and molecular level and much of the information collected is applicable to human cells. In addition to well-characterized embryonic stages, at least two different *Xenopus* cell lines are available for experimentation, namely, A6 kidney epithelial and XTC-2 cells. An increasing amount of information has accumulated with respect to the widely used A6 cell line. This immortal cell line was first isolated by Rafferty (1969) from proximal renal tubules of an adult male. A6 cells are fast growing and easily maintained in the laboratory. This cell line was used in a variety of

research studies examining genetic profiling under zero gravity, the function of Cystic Fibrosis transmembrane conductance regulator channels and the role of renal epithelial sodium channels in hypertension (Guerra, 2004; Ikuzawa, 2007; Ma, 2011; Niisato et al., 2012). Finally, these cells have been employed as a model system for the last 3 decades to study the regulation of *hsp* gene expression in response to proteasomal inhibitors and environmental stresses such as heat shock, sodium arsenite and cadmium chloride (Heikkila, 2010).

The *Xenopus* tissue culture (XTC-2) cell line is an embryonic cell line which was initially established by Pudney (1973) to study the growth of homeothermic vertebrate viruses. The XTC-2 cells have fibroblast morphology and are derived from *Xenopus* embryonic tissues (Pudney et al., 1973). XTC-2 cells were used extensively to examine the role of activin as a mesoderm-inducing factor in early amphibian embryogenesis (van den Eijnden-Van Raaij et al., 1990; Ariizumi et al.,1991; Spicer et al., 2010).

1.11 Heat Shock Response in *Xenopus laevis*

In general, the HSR in *Xenopus* is similar to the process reported in other model animal systems (Voellmy, 2004; Heikkila, 2010). However, although HSF1 in many systems is located within the cytoplasm, work with *Xenopus* oocytes revealed HSF1 bound to HSP90 in the nucleus (Ali et al., 1998). The presence of heat shock, cadmium and arsenite inducible HSF1-HSE binding activity in *Xenopus* was documented in several studies (Ovsenek and Heikkila, 1990; Karn et al., 1992; Gordon et al., 1997). Furthermore, the *Xenopus* HSF1 gene was cloned and the putative amino acid sequence revealed that it was similar in size to other vertebrate HSF1s and that the sequence identity was high with respect to the putative DNA binding, trimerization and C-terminal region containing a leucine zipper motif (Stumpf et al. 1995). Also, treatment of *Xenopus* cells with the HSF1 inhibitor, KNK437, inhibited HSP accumulation induced by heat

shock, sodium arsenite, cadmium chloride and proteasomal inhibitors (Manwell and Heikkila, 2007; Voyer and Heikkila, 2008; Young and Heikkila, 2010).

1.11.1 *Xenopus* HSP30

In *Xenopus laevis*, at least 5 intronless genes or gene fragments of the sHSP family, HSP30, have been isolated to date including *hsp30A, B, C, D* and part of *E* (Bienz, 1984; Krone et al., 1992). *Hsp30A* contains a 21 base-pair insertion, which includes a translational stop codon giving rise to a 10 kDa protein while *hsp30B* gene is a pseudogene (Bienz, 1984). *Hsp30C* and *hsp30D*, which were isolated and fully sequenced by Krone et al. (1992), encode two functional sHSPs, 24-kDa in size. Only a portion of the *hsp30E* gene was isolated so no additional information is available (Krone et al., 1992). In subsequent studies, *hsp30* genes were detected in chicken, fish and other amphibians but not in mammals (Norris et al., 1995; Helbing et al., 1996; Katoh et al., 2004; Elicker and Hutson, 2007). The number of *hsp30* genes within a family differs and is dependent on the species. For instance, at least 5 members were isolated in *Xenopus laevis* (Ohan and Heikkila, 1995; Tam and Heikkila, 1995), up to 18 isoforms were identified in *Poeciliid* fish (Norris et al., 1995) and as many as 10 were found in *Rana catesbeiana* (Helbing et al., 1996).

In *Xenopus*, *hsp*30 mRNA was detected constitutively and transiently in the cement gland of early and midtailbud stage embryos while HSP30 protein was found in late tailbud and older stages (Lang et al., 1999; Heikkila, 2003). In mammalian model systems, sHSPs were reported to inhibit apoptosis (Sun and MacRae, 2005). Since the cement gland disappears by means of apoptosis later in development, it was thought that HSP30 may prevent programmed cell death in this organ until HSP30 is degraded. During early development, *Hsp30C* was first heat-inducible at the late neurula/early tailbud stage, while *hsp30D* was not inducible until midtailbud as

determined by RNase protection and RT-PCR analysis (Krone et al., 1992; Ali et al., 1993; Ohan and Heikkila, 1995). Developmental regulation of heat-inducible *hsp30* gene expression may be controlled, at least in part, at the level of chromatin structure. For example pretreatment of embryos with histone deacetylase inhibitors (HDIs) resulted in premature expression of *hsp30* genes after the mid-blastula stage (Ovakim and Heikkila, 2003). It was likely that HDIs enhanced the acetylation of lysine residues of histone tails, which caused a loosening of chromatin conformation and allowed the DNA to become more accessible to transcription factors and RNA polymerase II.

In response to heat shock, HSP30 forms multimeric complexes with molecular masses ranging in size from 350-510 kDa (Ohan et al., 1998b). In vitro studies indicated that both HSP30C and D form multimeric complexes that bind to heat-induced unfolded protein and prevent them from forming aggregates (Abdulle et al., 2002). Furthermore, HSP30C and D multimeric complexes hold their client protein in a folding-competent state such that they can be refolded by other HSPs such as HSP70, in an ATP-dependent manner. In A6 cells, after the removal of heat stress the HSP30 multimeric complexes are phosphorylated which results in a breakdown of these multimeric complexes, changes in secondary structure and a loss of chaperone function (Fernando et al., 2003).

Various stressors including heat shock, cadmium chloride, sodium arsenite and proteasomal inhibitors induced HSP30 accumulation in A6 kidney epithelial cells. Stress-induced HSP30 accumulation in A6 cells was primarily cytoplasmic in a granular or punctuate pattern and localized in the perinuclear region as determined by immunocytochemistry and laser scanning confocal microscopy (Gellalchew and Heikkila, 2005).

1.11.2 *Xenopus* HSP70

In *Xenopus*, four *hsp*70 genes have been isolated: *hsp70A*, *hsp70B*, *hsp70C* and *hsp70D* (Bienz, 1984). Additionally, our laboratory isolated and characterized other members of the *hsp70* gene family including, *hsc*70.*I*, *hsc*70.*II* and *BiP* genes (Ali et al., 1996a; Ali et al., 1996b; Miskovic et al., 1997). The *hsp*70 genes are intronless and contain 3 HSEs in the 5' promoter region (Heikkila, 2010). During development, HSP70 was first heat-inducible after the mid-blastula transition (MBT), which marks the activation of the zygotic genome. The MBT is associated with the lengthening of the duration of the cell cycle, loss of synchronous cell division, a reduction in rate of DNA synthesis and transcription of certain embryonic genes, like *hsp*70 (Heikkila et al., 1997). In A6 cells, our laboratory reported that a number of stressors induced HSP70 accumulation including heat shock, sodium arsenite, herbimycin A, hydrogen peroxide, ethanol, proteasomal inhibitors and cadmium chloride (Darasch et al., 1988; Briant et al., 1997; Heikkila, 2004; Muller et al., 2004; Woolfson and Heikkila, 2009; Young et al., 2009); Young and Heikkila, 2010). Recently, it was reported that different proteasomal inhibitors including MG132, lactacystin, celastrol, curcumin and withaferin A induced the accumulation of HSP30 as well as HSP70 (Young and Heikkila, 2010; Walcott and Heikkila, 2010; Khan and Heikkila, 2011; Khan et al., 2012).

1.11.3 Effect of Sodium Arsenite and Cadmium Chloride on HSP Accumulation in *Xenopus*

As mentioned previously, sodium arsenite and cadmium chloride were reported to induce HSP30 and HSP70 accumulation in *Xenopus* (Gellalchew and Heikkila, 2005; Voyer and Heikkila, 2008; Young et al., 2009; Brunt et al., 2012). Immunocytochemical analysis revealed that arsenite or cadmium-induced HSP30 accumulation occurred primarily in the cytoplasm in a granular pattern, with slightly larger HSP30 staining structures also present (Voyer and Heikkila,

2008; Woolfson and Heikkila, 2009). Recent studies by Brunt et al. (2012) determined that treatment of A6 cells with sodium arsenite or cadmium chloride caused an inhibition of proteasomal activity as evidenced by an increase in the accumulation of ubiquitinated protein and an inhibition in CT-like enzyme activity. Interestingly, the addition of a mild heat shock further enhanced HSP30 and HSP70 accumulation in A6 cells treated with sodium arsenite or cadmium chloride (Woolfson and Heikkila, 2009; Young et al., 2009). It was suggested that treatment of A6 cells with a mild heat shock or low concentration of sodium arsenite or cadmium chloride does not cause sufficient protein unfolding or misfolding to initiate a strong activation of HSF1. However, combining the stress induces unfolded protein to accumulate and exceed a critical intracellular level or set-point to induce a major activation of HSF1. The possibility of a HSF1 set-point has been described in a number of systems including mouse T-lymphocytes and testis, intertidal mussels, HeLa cells and *Xenopus* heart (Sarge 1995; Lee et al., 1995; Ali et al., 1997; Buckley et al., 2001; Gothard et al., 2003).

1.12 Objectives

The main goal of this thesis was to investigate the possible synergistic effect of sodium arsenite and cadmium chloride on HSP accumulation in *Xenopus laevis* A6 kidney epithelial cells. While earlier studies examined the effect of a single chemical stressor on HSP accumulation, relatively few have investigated the impact of combined chemical stressors. *Xenopus*, like other aquatic organisms, can be exposed to various chemical stressors simultaneously in their natural environment. The present study examined the effects of sodium arsenite and cadmium chloride on HSP accumulation since these stressors are widespread environmental contaminants that have been associated with various diseases and cytotoxic effects at the cellular level. The specific objectives are as follows:

1. To examine the effect of low concentrations of sodium arsenite and cadmium chloride both singly and in combination on HSP30 and HSP70 accumulation.

2. To assess if combined sodium arsenite- and cadmium chloride-induced HSP30 and HSP70 accumulation is mediated via HSF1 activation using the HSF1 inhibitor, KNK437.

3. To determine the effect of sodium arsenite and cadmium chloride on intracellular localization and pattern of HSP30 accumulation via immunocytochemistry and laser scanning confocal microscopy.

4. To determine if the addition of a mild heat shock can further enhance the accumulation of HSP30 and HSP70 induced by combined sodium arsenite and cadmium chloride treatment.

5. To examine the effect of combined sodium arsenite and cadmium chloride treatment on the relative level of ubiquitinated protein.

2. Materials and Methods

2.1 Maintenance and treatment of *Xenopus laevis* cells

Xenopus laevis A6 kidney epithelial cells were obtained from the American Type Culture Collection (Rockville, MD), and *Xenopus laevis* tissue culture (XTC-2) cells were a gift from Dr. Mungo Marsden (University of Waterloo, ON). Both cell lines were grown in 70% Leibovitz L-15 Media containing 10% fetal bovine serum and 1% penicillin/streptomycin (Sigma-Aldrich, Oakville, ON) at 22 ºC in T-75 cm² flasks (VWR). After cells reached confluence, old media was aspirated and 1 mL versene [0.02% (w/v) KCl, (0.8% (w/v) NaCl, 0.02% (w/v) KH2PO4, 0.115% (w/v) Na2HPO4, 0.02% (w/v) Na2EDTA] was added, and then removed. This was followed by a second wash of 2 mL versene for 1 min, which was aspirated. Subsequently, 1 mL of 1X trypsin (Sigma-Aldrich) in 100% Hanks balanced salt solution (HBSS; Sigma-Aldrich) for 1 min was added to detach the cells from the bottom of the flask. Cells were resuspended in fresh media and evenly distributed into new culture flasks.

Flasks reaching at least 90% confluence were used for treatments. Heat shock treatment of cells were performed in water baths set to 33 or 35 °C for 2 h followed by a 2 h recovery at 22 °C. Sodium arsenite (Sigma-Aldrich) was dissolved in sterile distilled water to make a stock solution of 100 mM, from which a 1 mM working solution was created. Cadmium chloride (Sigma-Aldrich) was dissolved in sterile distilled water to make a stock solution of 100 mM, from which an additional 1 mM working solution was made. MG132 (Sigma-Aldrich) and KNK437 (Calbiochem; Gibbstown, NJ) were dissolved in dimethylsulphoxide (Sigma-Aldrich) to prepare 5 mg/mL stock solutions. MG132 and KNK437 treatments of cells employed final concentrations of 30 μM MG132 and 100 μM KNK437, respectively. Treatments with KNK437 were performed 6 h prior to treatment with sodium arsenite and cadmium chloride. Cell

morphology was recorded using a phase contrast Nikon TMS microscope equipped with a Nikon Coolpix 995 digital camera (400X magnification).

2.2 Protein Isolation and Quantification

At the conclusion of the treatments, the media was removed from the flasks followed by rinsing of the cells with 2 mL of 65% HBSS to the cells and the subsequent addition of 1 mL of 100% HBSS. A cell scraper was used to remove cells from the flask, which were then transferred to a 1.5 mL microcentrifuge tube. The cells were centrifuged at 14, 000 rpm for 1 min. The supernatant was removed and cells were stored at -80 °C until protein isolation. Protein was isolated using 300 µL lysis buffer (200 mM sucrose, 2 mM EGTA, 1 mM EDTA, 40 mM NaCl, 30 mM HEPES, pH 7.4), which contained 1% SDS, 1% protease inhibitor. For ubiquitinated protein, 10 mM N-ethylmaleimide (Sigma-Aldrich) was added to the lysis buffer to inhibit ubiquitin conjugating enzymes. Next, samples were sonicated on ice with a sonic dismembranator (Model 100, Fisher Scientific; Waltham) and then centrifuged at 14,000 rpm for 30 min at 4 ºC. The protein supernatant was then isolated and stored in the -20 ºC until further use.

The bicinchoninic acid (BCA) method was used for protein quantification according to the manufacturer's instructions (Pierce, Rockford, IL). A protein standard was made using a bovine serum albumin (BSA; Bioshop; Burlington, ON). BSA was diluted in distilled water to concentrations ranging from 0 to 2 mg/mL. Protein samples in 1.5 mL microcentrifuge tubes were diluted to a concentration of 1:2 in distilled water. BSA standards and protein samples in 10 µL volumes were loaded into each well, in triplicate, into a 96 well polystyrene plate. Eighty µL of BCA reagent A and B (Pierce) was added to each standard and protein sample and the plate was incubated at 37 °C for 30 min. Subsequently, the plate was read at 562 nm using a

Versamax Tunable microplate reader (Molecular Devices, Sunnyvale, CA, USA) and Softmax Pro software. A standard curve was created using the BSA protein standards which was used to determine the concentration of the protein samples.

2.3 SDS-Polyacrylamide gel electrophoresis

Protein separation by sodium dodecyl sulfate-polyacrylamide gel electrophoresis (SDS-PAGE) employed 12% gels for HSP30, HSP70 and actin and 10% gels for ubiquitinated protein. Separating gels [10 or 12% (w/v) acrylamide, 0.32% (v/v) n'n'-bis methylene acrylamide, 0.375 M Tris pH 8.8, 1% (w/v) SDS, 0.2% (w/v) ammonium persulfate (APS), 0.14% (v/v) tetramethylethylenediamine (TEMED)] were prepared and allowed to polymerize for 25 min after 100% ethanol was layered on top of the gel. Once the separating gel solidified, ethanol was removed and the stacking gel [4% (v/v) acrylamide, 0.11% (v/v) n'n'-bis methylene acrylamide, 0.125 M Tris pH 6.8, 1% (w/v) SDS, 0.4% (w/v) APS, 0.21% (v/v) TEMED] was added. Combs were inserted to create lanes in the stacking gel after which it was left to polymerize for another 25 min. Protein samples of 30 μg of protein for HSP30, HSP70 and actin or 60 μg for ubiquitinated protein were added to loading buffer [0.0625 M Tris pH 6.8, 10% (v/v) glycerol, 2% (w/v) SDS, 5% (v/v) β-mercaptoethanol, 0.00125% (w/v) bromophenol blue]. Samples were boiled for 10 min, cooled, briefly centrifuged and loaded on to the gel. Gels were electrophoresed in 1 X running buffer [25 mM Tris, 0.2 M glycine, 1 mM SDS] at 90 V until samples reached the separating gel at which point the voltage was increased to 140 V for ubiquitinated protein or 160 V for HSP30, HSP70 and actin.

2.3.1 Immunoblotting

Nitrocellulose membranes (BioRad, Mississauga, ON) and filter paper (BioRad) were cut to a size of 5.5 X 8.5 cm. Membranes were soaked for 30 min in 10% transfer buffer [25 mM Tris, 192 mM glycine, 10% (v/v) methanol], for ubiquitin blots, or 20% transfer buffer [25 mM Tris, 192 mM glycine, 20% (v/v) methanol], for HSP30, HSP70 and actin. Once electrophoresis was finished, the stacking gel was removed and the remainder of the gel was soaked in transfer buffer for 15 min. Protein was transferred to the nitrocellulose membrane with a Trans-Blot Semi-dry Transfer cell (BioRad) for 25 min at 20 V. Once the transfer was complete, membranes were stained with Ponceau-S stain [0.19% (w/v) Ponceau-S, 5% (v/v) acetic acid] for 10 min to determine the quality of the transfer and loading of protein. Blots were rinsed with distilled water and scanned. Membranes were then incubated with 5% blocking [20 mM Tris pH 7.5, 0.1% Tween 20 (Sigma), 300 mM NaCl, 5% (w/v) Nestle® Carnation skim milk powder] solution for 1 h to prevent non-specific binding. Once the blocking solution was removed, the membranes were incubated with rabbit anti- *Xenopus* HSP30 (1:500), rabbit anti-*Xenopus* HSP70 (1:350; Abgent, San Diego, CA) or rabbit anti-actin (1:200; Sigma) polyclonal antibodies diluted in 5% blocking solution and left overnight. For ubiquitinated protein, membranes were incubated overnight with a mouse anti-ubiquitin (1:150; Invitrogen, Carlsbad, CA) monoclonal antibody diluted in 5% bovine serum albumin (BSA; Fisher Scientific). After incubation with primary antibody, membranes were washed once for 15 min and twice for 10 min, with 1X TBS-T [20mM Tris, 300 mM NaCl, (pH 7.5), 0.1% (v/v) Tween 20]. Membranes were then incubated with secondary antibody in blocking solution for 1 h. AP-conjugated goat-anti-rabbit (BioRad) at a dilution of 1:3000 dilution for HSP30, HSP70, actin and AP-conjugated goat-anti-mouse (BioRad) at a 1:1000 dilution were used. Following incubation with secondary antibody, the

membranes were washed once for 15 min with TBS-T and twice for 5 min. Membranes were then washed in alkaline phosphatase detection buffer [50 mM Tris, 50 mM NaCl, 25 mM $MgCl_2$ pH 9.5, 0.3% 4-nitro blue tetrazolium (Roche) and 0.17% 5-bromo-4-chloro-3-indolyl phosphate, toluidine salt (Roche) until bands or ubiquitinated protein lanes were visible and then detection buffer was removed and the blots were rinsed with distilled water. The blots were then scanned.

2.4 Densitometry and Statistical Analysis

Image J software (Version 1.46; National Institute of Health http://rsb.info.nih.gov/ij/) was used to perform densitometric analysis on all blots performed in triplicate. The average densitometric values were expressed and graphed as a percentage of the maximum HSP30 or HSP70 bands or as a percentage of treatment without pretreatment with KNK437. The standard error is represented by vertical error bars. To determine if any statistically significant differences existed between samples, a one-way ANOVA with a Tukey's post-test was performed on the data. Confidence levels used were 95% ($p < 0.05$;*).

2.5 Immunocytochemistry and Laser Scanning Confocal Microscopy

A6 cells were grown on flame sterilized 22 x 22 mm base-washed glass coverslips in sterile Petri dishes. Coverslips were washed with a base solution [49.5% (v/v) ethanol, 0.22 M NaOH] in small staining jars (Thomas Scientific Apparatus, Philadelphia, PA, USA) for 30 min and then rinsed with distilled water for 3 h. Following treatment, L-15 media was removed and cells were rinsed twice with phosphate buffered saline (PBS; 1.37 M NaCl, 67 mM Na_2HPO_4, 26 mM KCl, 14.7 mM H_2PO_4, 1 mM $CaCl_2$, 0.5 mM $MgCl_2$ pH 7.4). Once washed, coverslips were transferred to small Petri dishes and fixed with 3.7% paraformaldehyde (BDH, Toronto, ON) for 15 min. A6 cells were then rinsed with three 5 min each washes with PBS and then

permeabilized using 0.3% Triton X-100 (Sigma) for 10 min. After an additional three washes with PBS, A6 cells were incubated with 3.7 % (w/v) bovine serum albumin fraction V (BSA fraction V; Fischer Scientific) for 1 h or overnight at 4 °C. Subsequently, coverslips were incubated with affinity-purified rabbit anti-*Xenopus* HSP30 antibody (1:500) in 3.7% BSA for 1 h. After three washes for 3 min each with PBS, indirect labeling of cells was carried out with a fluorescent-conjugated secondary antibody, goat anti-rabbit Alexa Fluor 488 (Invitrogen Molecular Probes) at a 1:2000 dilution in 3.7% BSA for 30 min in the dark. Coverslips were then incubated with rhodamine-tetramethylrhodamine-5-isothiocyanate phalloidin (TRITC; Invitrogen Molecular Probes) for 15 min at a 1:100 in 3.7% BSA in the dark in order to visualize the actin cytoskeleton. Coverslips were dried and mounted on a glass microscope slide with Vectashield (Vector Laboratories Inc., Burlingame, CA) containing 4,6-diamidino-2-phenylindole (DAPI; Vector Laboratories Inc.) to stain nuclei followed by three washes of 5 min each. Clear nail polish was used to permanently attach coverslips to glass slides and the slides were stored at 4 °C. Slides were examined using a Zeiss Axiovert 200 confocal microscope with LSM 510 META software (Carl Zeiss Canada Ltd., Mississauga, ON).

3. Results

3.1 Comparison of stress-induced HSP30 accumulation in A6 cells and XTC-2 cells

Initial studies compared the heat shock response of A6 cells and XTC-2 cells to determine the optimal cell line for use in this study. HSP30 accumulation was employed as the key criteria since the anti-*Xenopus* HSP30 antibody can be used for both immunoblot and immunocytochemical analysis. As shown in Figure 3, heat-shock treatment at 33 and 35 °C with a 2 h recovery at 22 °C resulted in a greater accumulation of HSP30 in A6 cells compared to XTC-2 cells. Furthermore, treatment with 20, 30 and 50 µM sodium arsenite for 18 h resulted in a significantly higher accumulation of HSP30 in A6 cells than found with XTC-2 cells (Fig.4). The relative levels of total actin (G- and F-actin) remained constant in both experiments. Thus, A6 cells were chosen to investigate the effect heavy metals on HSP accumulation.

3.2 Effect of various heavy metals on HSP30 accumulation in A6 cells

In the next set of preliminary experiments, I examined the effect of different heavy metals, namely zinc sulfate, lead nitrate and copper sulfate on HSP30 accumulation in A6 cells. The concentrations of heavy metals employed in this study have been shown to induce HSP accumulation in amphibian and/or mammalian systems (Hatayama et al., 1993; Murata et al., 1999; Gellalchew and Heikkila, 2005; Gaitanaki et al., 2006; Young et al., 2009; Woolfson and Heikkila, 2009). As shown in Figure 5A and 6A, A6 cells exposed to heat shock induced a relatively high accumulation of HSP30, whereas treatment of cells with 100, 200, 300 or 500 µM zinc sulfate or 5, 10, 25 and 50 µM lead nitrate for 8 h did not produce detectable levels of HSP30. Additionally, phase-contrast microscopy revealed that cells treated with 100 or 200 µM zinc sulfate or 50 µM lead nitrate had morphology that was

Figure 3. Comparison of heat shock-induced HSP30 accumulation in A6 and XTC-2 cells. A6 and XTC-2 cells were maintained at 22 °C (C) or incubated at 33 or 35 °C for 2 h with a 2 h recovery at 22 °C. Total protein was isolated and immunoblot analysis was performed employing a rabbit polyclonal anti-*Xenopus* HSP30, or an anti-actin antibody as detailed in Materials and methods. The low level of HSP30 in the A6 control lane was due to spill over of protein from the adjacent well. These results are representative of 2 different experiments.

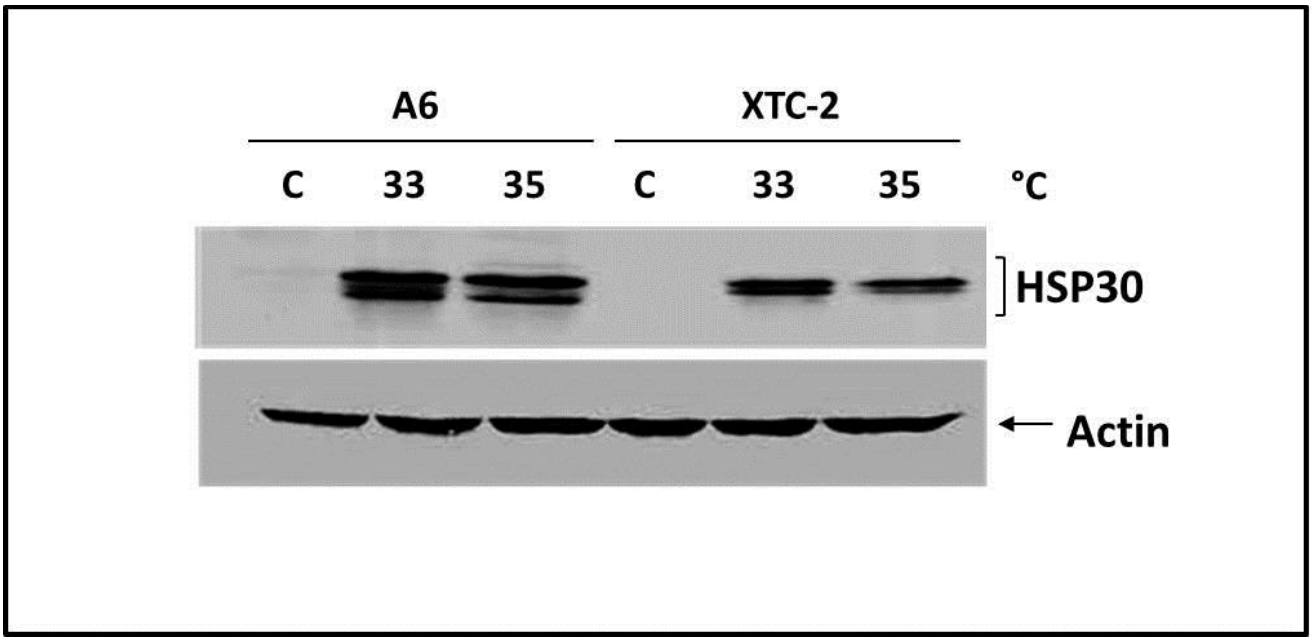
A6
XTC-2
C
33
35
C
33
35
°C
HSP30
Actin

Figure 4. Comparison of the effect of sodium arsenite on HSP30 accumulation in A6 and XTC-2 cells. A6 and XTC-2 cells were maintained at 22 °C (C) or exposed to 20, 30 or 50 µM sodium arsenite (As) for 18 h at 22 °C. Immunoblot analysis of isolated total protein to detect the relative levels of HSP30 and actin was performed as detailed in Materials and methods. The weak HSP30 signal detected for both the A6 and XTC-2 control lanes was due to spill over of protein from the adjacent wells. These results are representative of 2 different experiments.

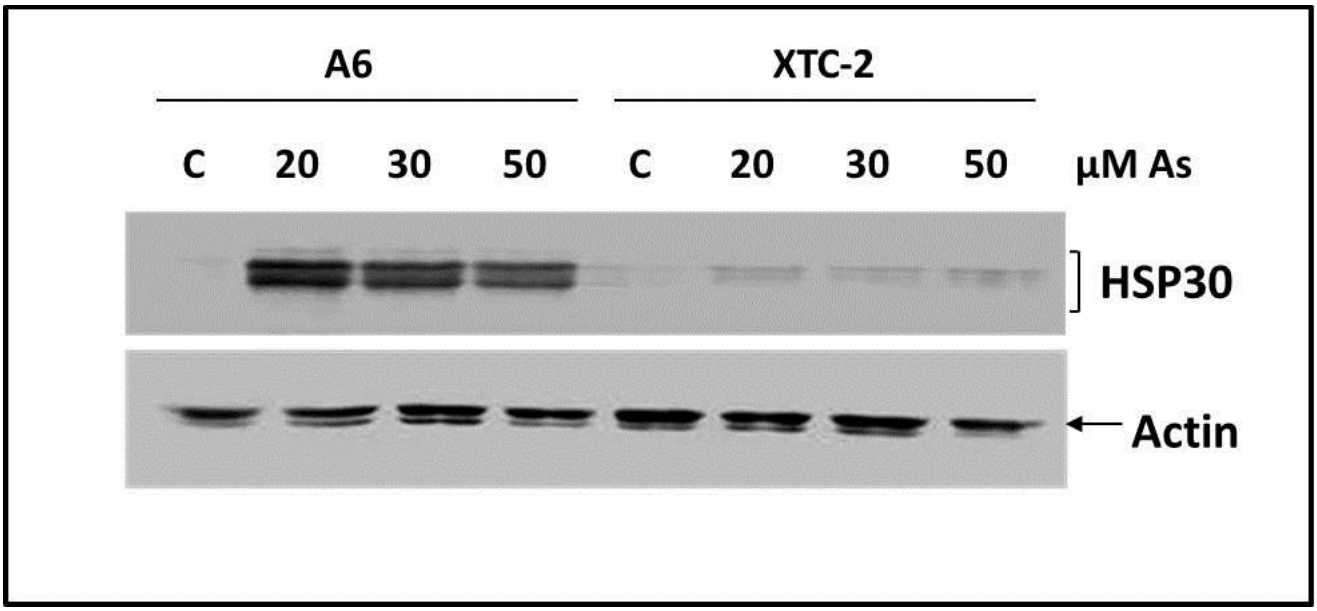
A6
XTC-2
C
20
30
50
C
20
30
50
μM As
HSP30
Actin

Figure 5. Effect of zinc sulfate on HSP accumulation and cell morphology in A6 cells. A) Cells were maintained at 22 °C (C), incubated at 33 °C or exposed to 100, 200, 300 or 500 µM zinc sulfate ($ZnSO_4$) for 8 h at 22 °C. Immunoblot analysis of isolated total protein to detect the relative levels of HSP30 and actin was performed as detailed in Materials and methods. These results are representative of 2 different experiments. B) Phase contrast microscopy was employed to examine the morphology of cells treated with zinc sulfate. A6 cells were photographed using a Nikon Coolpix 995 digital camera (400X magnification).

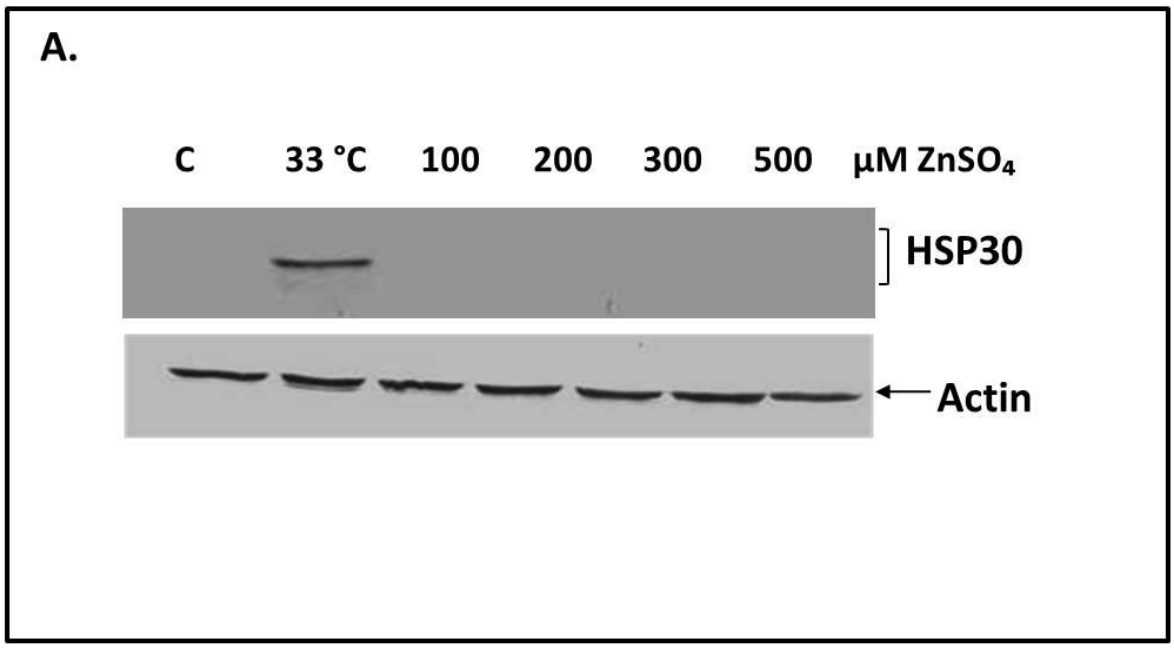
A.
C
33 °C
100
200
300
500
µM ZnSO4
HSP30
Actin

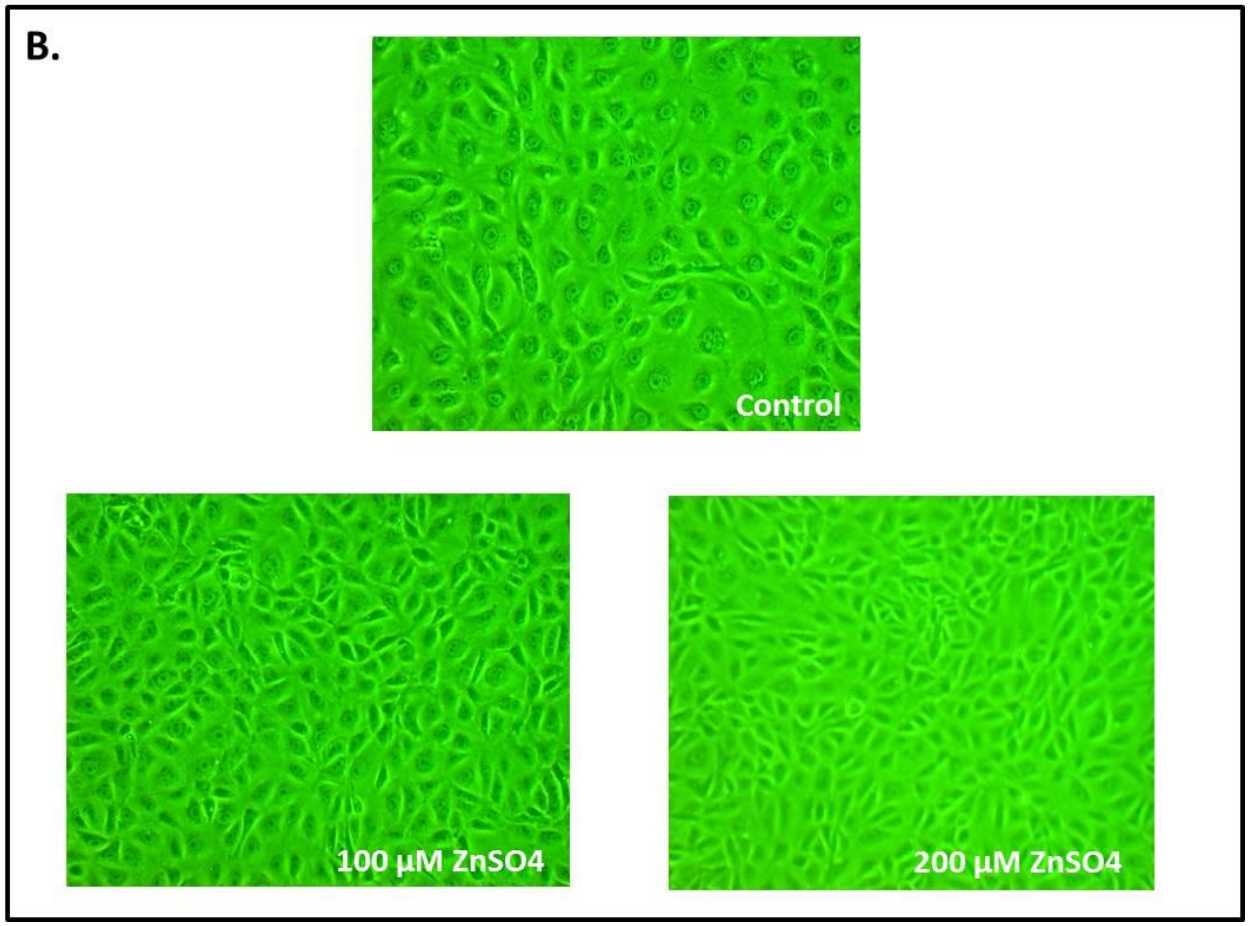
B.
Control
100 µM ZnSO4
200 µM ZnSO4

Figure 6. Effect of lead nitrate on HSP accumulation and cell morphology in A6 cells. A) Cells were maintained at 22 °C (C), incubated at 33 °C or exposed to 5, 10, 25 or 50 μM lead nitrate ($Pb(NO_3)_2$) for 8 h at 22 °C. Immunoblot analysis of isolated total protein to detect the relative levels of HSP30 and actin was performed as detailed in Materials and methods. These results are representative of 2 different experiments. B) Phase contrast microscopy was employed to examine the morphology of cells treated with lead nitrate. A6 cells were photographed using a Nikon Coolpix 995 digital camera (400X magnification).

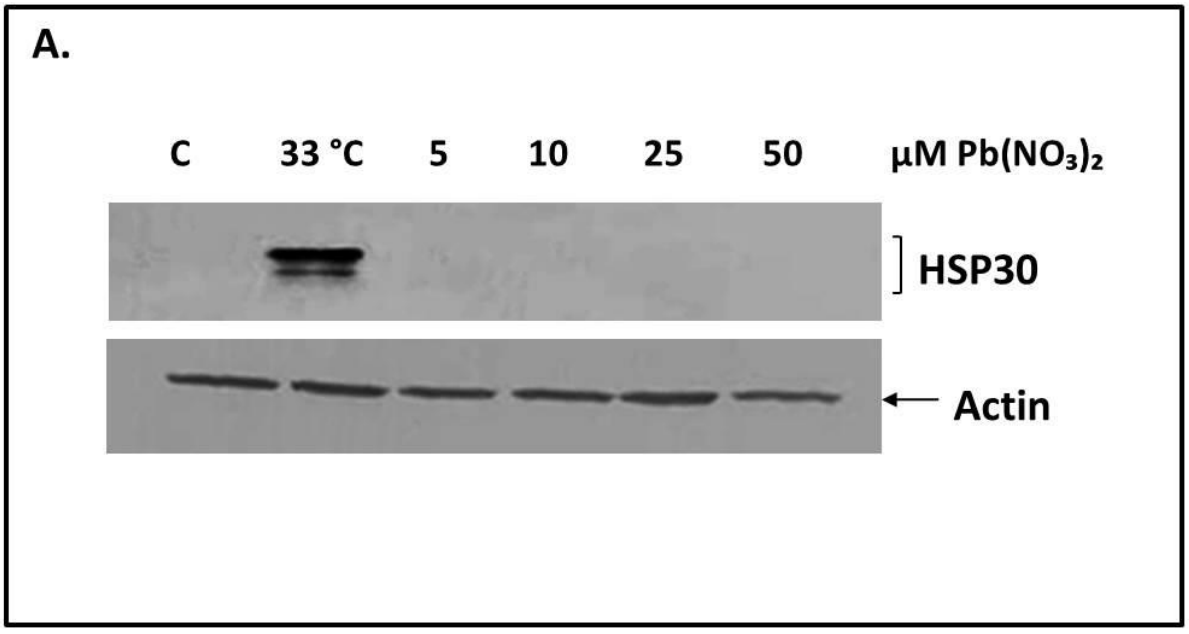
A.
C
33 °C
5
10
25
50
µM Pb(NO3)2
HSP30
Actin

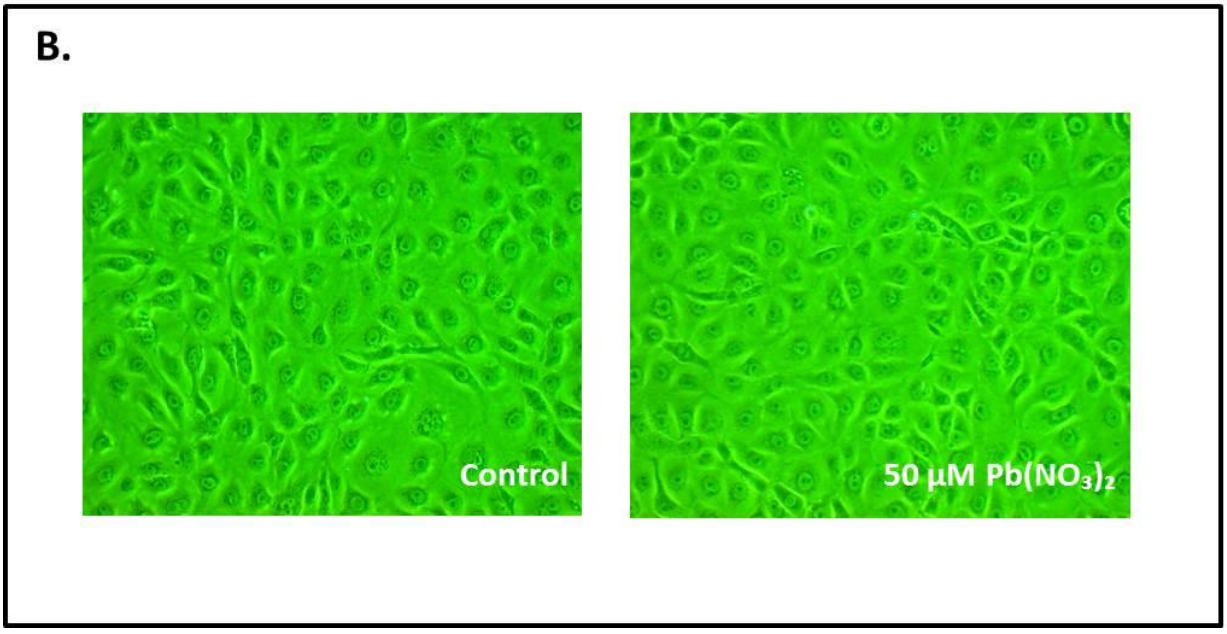
B.
Control
50 µM Pb(NO3)2

comparable to control cells (Fig. 5B and 6B). Treatment of A6 cells with copper sulfate did not result in detectable HSP30 accumulation at concentrations ranging from 100 to 500 μM although a weak accumulation of HSP30 was observed at 1,000 μM (Fig. 7A). While a control-like morphology was observed at lower concentrations of copper sulfate, treatment of cells with 1,000 μM of this metal resulted in cells having an elongated structure with long processes as well as a lower overall density (Fig. 7B). Given these results with zinc, lead and copper, subsequent studies employed sodium arsenite and cadmium chloride, which were shown previously to enhance HSP accumulation in A6 cells.

3.3 Effect of simultaneous sodium arsenite and cadmium chloride treatment on HSP30 and HSP70 accumulation in A6 cells

The effect of different concentrations of sodium arsenite and cadmium chloride, either individually or combined, on HSP30 and HSP70 accumulation as well as cell morphology in A6 cells were investigated. Treatment of cells with 10 μM sodium arsenite, 10 or 50 μM cadmium chloride for 12 h resulted in minimal or non-detectable levels of HSP30 and HSP70, while a greater accumulation of HSPs was observed after treatment of 100 μM. Interestingly, combined stressor treatments produced large increases in the relative levels of HSP30 and HSP70 compared to the stressors individually, as seen in Figure 8A. Densitometric analysis revealed that treatment of cells with 10 μM sodium arsenite plus 50 μM cadmium chloride resulted in a 12-fold and 5-fold increase in HSP30 and HSP70, respectively, compared to the sum of the responses obtained with each of the individual stressors (Fig. 8B).

Figure 7. Effect of copper sulfate on HSP accumulation and cell morphology in A6 cells. A) Cells were maintained at 22 °C (C), incubated at 33 °C or exposed to 100, 200, 300, 500 or 1000 µM copper sulfate ($CuSO_4$) for 8 h at 22 °C. Immunoblot analysis of isolated total protein to detect the relative levels of HSP30 and actin was performed as detailed in Materials and methods. These results are representative of 2 different experiments. B) Phase contrast microscopy was employed to examine the morphology of cells subjected to copper sulfate treatment. A6 cells were photographed using a Nikon Coolpix 995 digital camera (400X magnification).

\

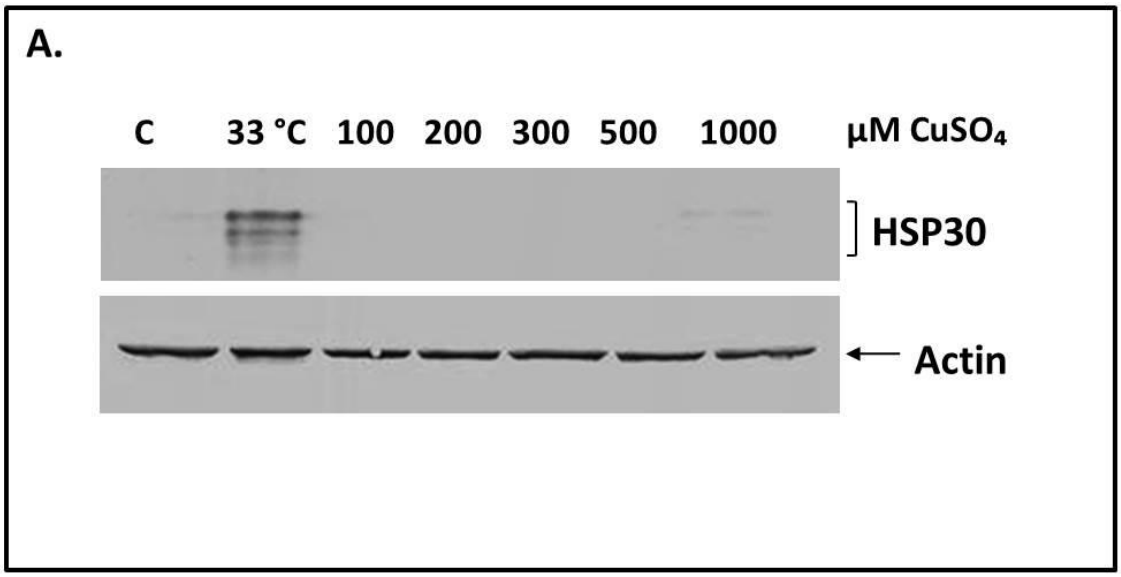
A.
C
33 °C
100
200
300
500
1000
µM CuSO4
HSP30
Actin

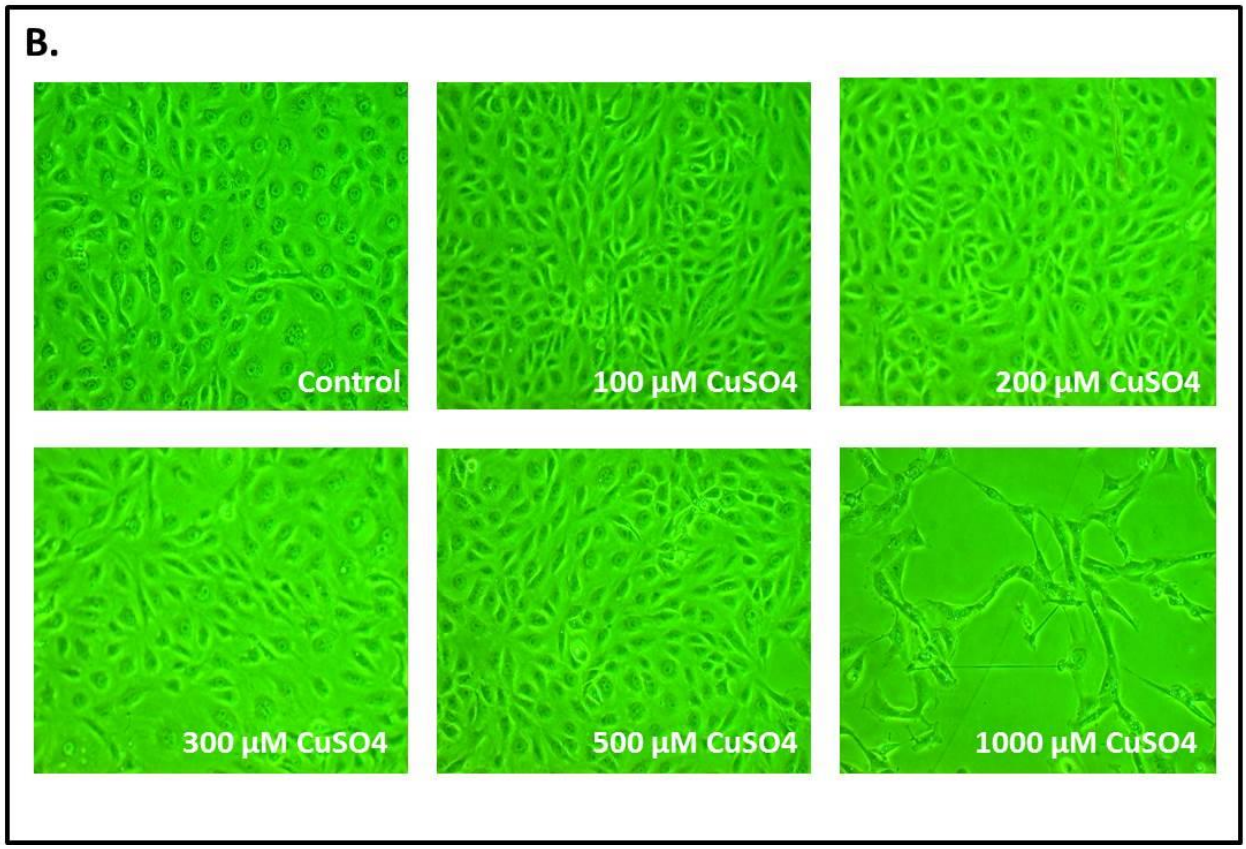
B.
Control
100 µM CuSO4
200 µM CuSO4
300 µM CuSO4
500 µM CuSO4
1000 µM CuSO4

Figure 8. Enhanced accumulation of HSP30 and HSP70 after a 12 h concurrent exposure to 10 μM sodium arsenite plus 10, 50 or 100 μM cadmium chloride. A) Cells were maintained at 22 °C for 12 h (C) or exposed to 10 μM sodium arsenite (As) and/or 10, 50 or 100 μM cadmium chloride (Cd) for 12 h. Total protein was isolated and the relative levels of HSP30, HSP70 and actin were detected by immunoblot analysis as described in Materials and methods. B) Image J (Version 1.46) software was utilized to perform densitometric analysis of HSP30 (white bars) and HSP70 (black bars) from 5 different experiments. Results were expressed as a percentage of the maximum hybridization signal obtained for each protein (10 μM sodium arsenite plus 100 μM cadmium chloride for HSP30 and HSP70). Error bars represent standard error. Significant differences compared to control are indicated as * ($p < 0.05$).

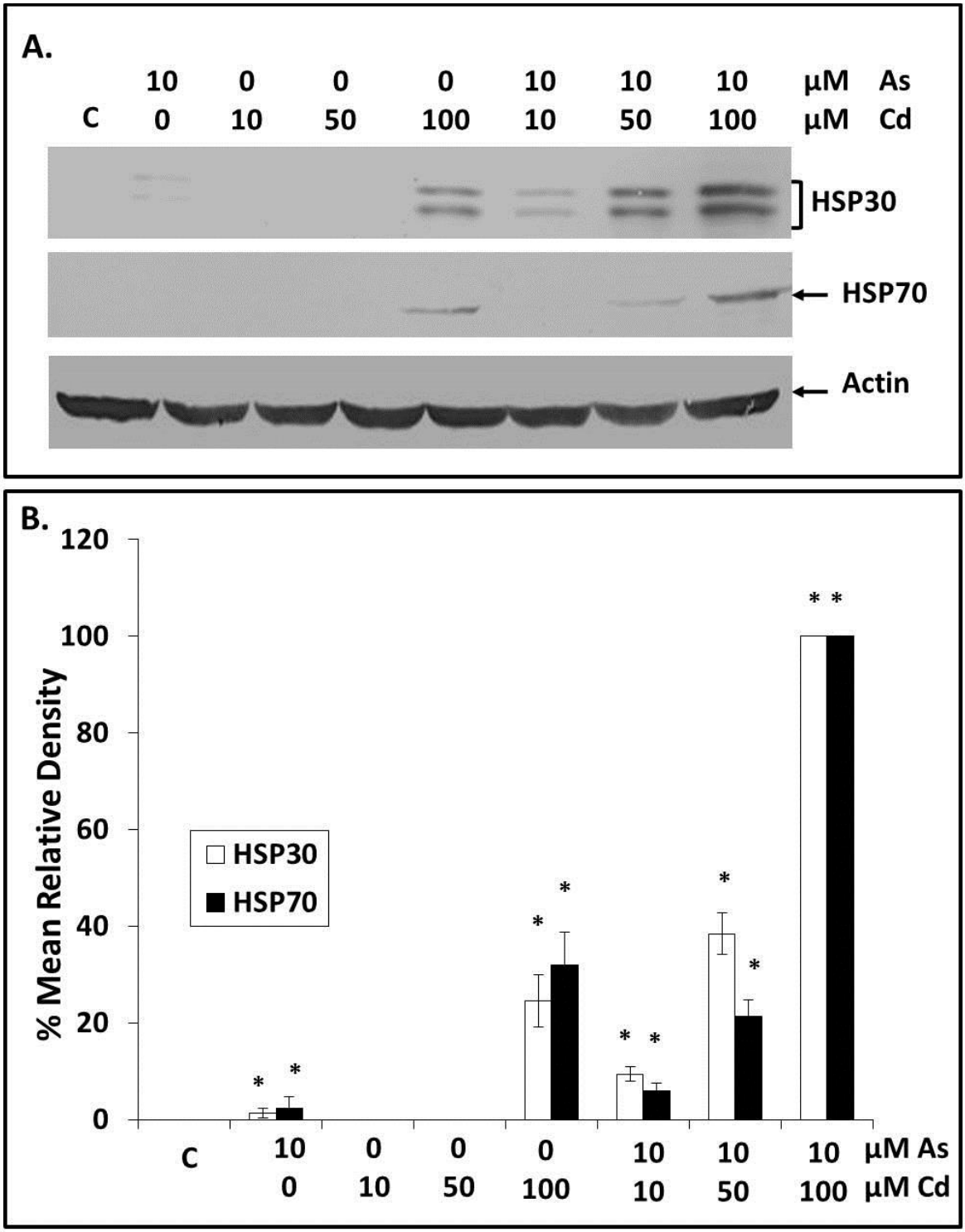
A.
C
10 0
0 10
0 50
0 100
10 10
10 50
10 100
µM As
µM Cd
HSP30
HSP70
Actin
B.
% Mean Relative Density
120
100
80
60
40
20
0
HSP30
HSP70
C
10 0
0 10
0 50
0 100
10 10
10 50
10 100
µM As
µM Cd

Cells treated with combined 10 μM sodium arsenite and 100 μM cadmium chloride for 16 h validated previous results of significant HSP30 and HSP70 accumulation in combined stressor treatments as shown in Figure 9A. Densitometric analysis in Figure 9B confirmed a synergistic action between chemical stressors which is not exclusive to only 12 h treatment times. Throughout these experiments the relative levels of actin remained constant. Treatment of A6 cells with 10 μM sodium arsenite, 10, 50 or 100 μM cadmium chloride, or exposure to 10 μM sodium arsenite plus 10 or 50 μM cadmium chloride for 16 h had morphology comparable to control cells (Fig. 10). However, cells treated with 10 μM sodium arsenite plus 100 μM cadmium chloride resulted in a lower density of cells and some cells having a rounder appearance. Time course studies of the three combined sodium arsenite and cadmium chloride treatments revealed that detectable accumulation of HSP30 and HSP70 occurred at 8 h with increased relative levels at 16 and 24 h (Fig. 11). However, extending treatment times to 48 h resulted in a decrease in HSP30 and HSP70 accumulation relative to 24 h levels (Fig. 12).

In the next series of experiments, cells were treated with a fixed concentration of 50 μM cadmium chloride plus either 2.5 or 5 μM sodium arsenite for 12 h. As shown in Figure 13A, treatment of cells with either 50 μM cadmium chloride or 2.5 μM sodium arsenite alone did not induce detectable HSP accumulation whereas exposure of cells to 5 μM sodium arsenite produced a low level of HSP30 but no detectable HSP70. However, the concurrent exposure of cells to 2.5 or 5 μM sodium arsenite plus 50 μM cadmium chloride resulted in enhanced HSP30 accumulation, which was confirmed by the densitometry in Figure 13B. Increased relative levels of HSP70 were only found in cells treated with 5 μM sodium arsenite plus 50 μM cadmium chloride.

Figure 9. Effect of a 16 h concurrent sodium arsenite and cadmium chloride treatment on HSP30 and HSP70 accumulation. A) Cells were maintained at 22 °C (C) or exposed to 10 μM sodium arsenite (As) and/or 100 μM cadmium chloride (Cd). Total protein was isolated and HSP30, HSP70 and actin was detected by immunoblot analysis as described in Materials and methods. B) Densitometric analysis of HSP30 (white bars) and HSP70 (black bars) of 3 separate experiments was performed as described in Materials and methods and the results are expressed as a percentage of the maximum signal obtained for each protein (10 μM sodium arsenite plus 100 μM cadmium chloride for HSP30 and HSP70). Error bars represent standard error. Significant differences compared to control are indicated as * ($p < 0.05$).

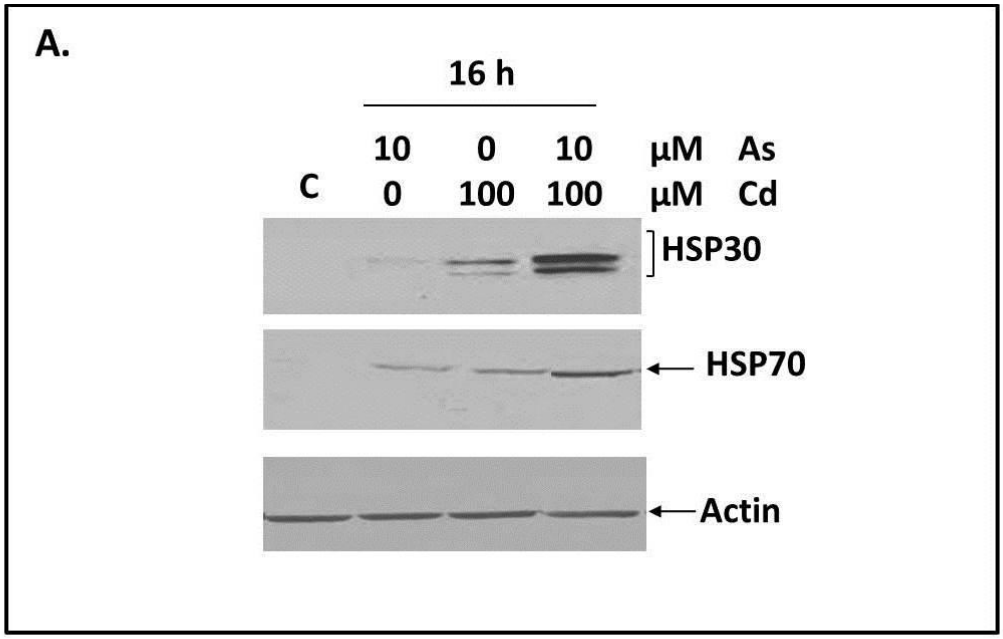
A.
16 h
C
10
0
10
µM As
0
100
100
µM Cd
HSP30
HSP70
Actin

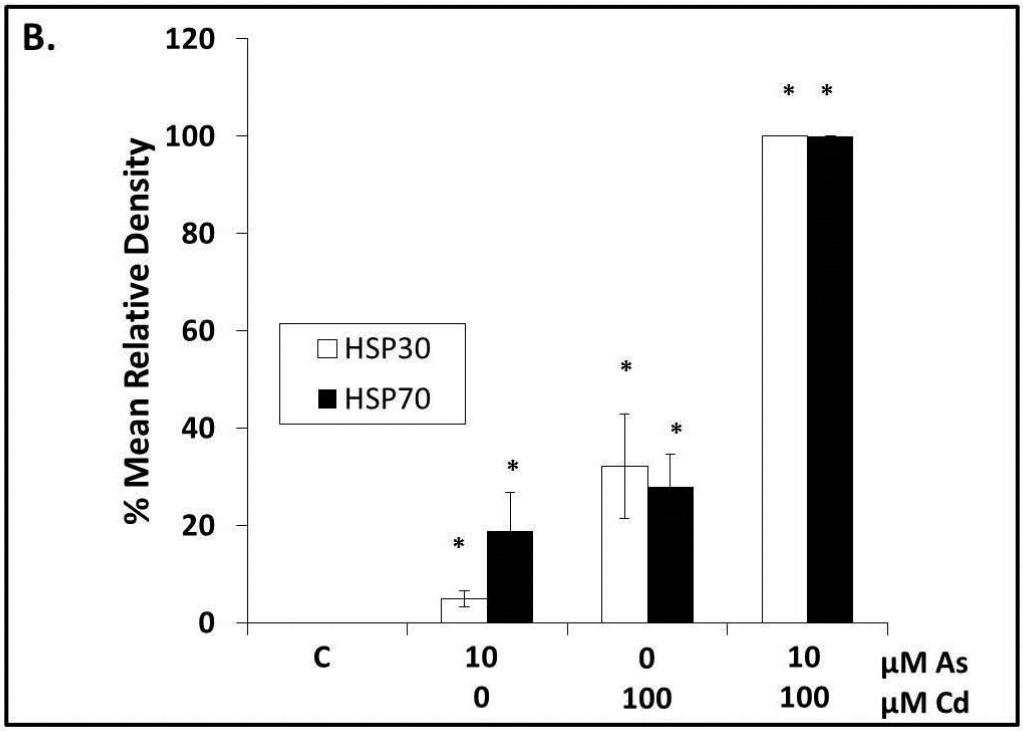
B.
% Mean Relative Density
120
100
80
60
40
20
0
HSP30
HSP70
C
10
0
0
100
10
100
µM As
µM Cd

Figure 10. Effect of sodium arsenite and/or cadmium chloride on A6 cell morphology. A) Cells were maintained at 22 °C for 16 h (control) or exposed to 10 μM sodium arsenite (As) and/or 10, 50 or 100 μM cadmium chloride (Cd) for 16 h. Phase contrast microscopy was employed to examine the morphology of cells subjected to sodium arsenite and/or cadmium chloride treatment. A6 cells were photographed using a Nikon Coolpix 995 digital camera (400X magnification).

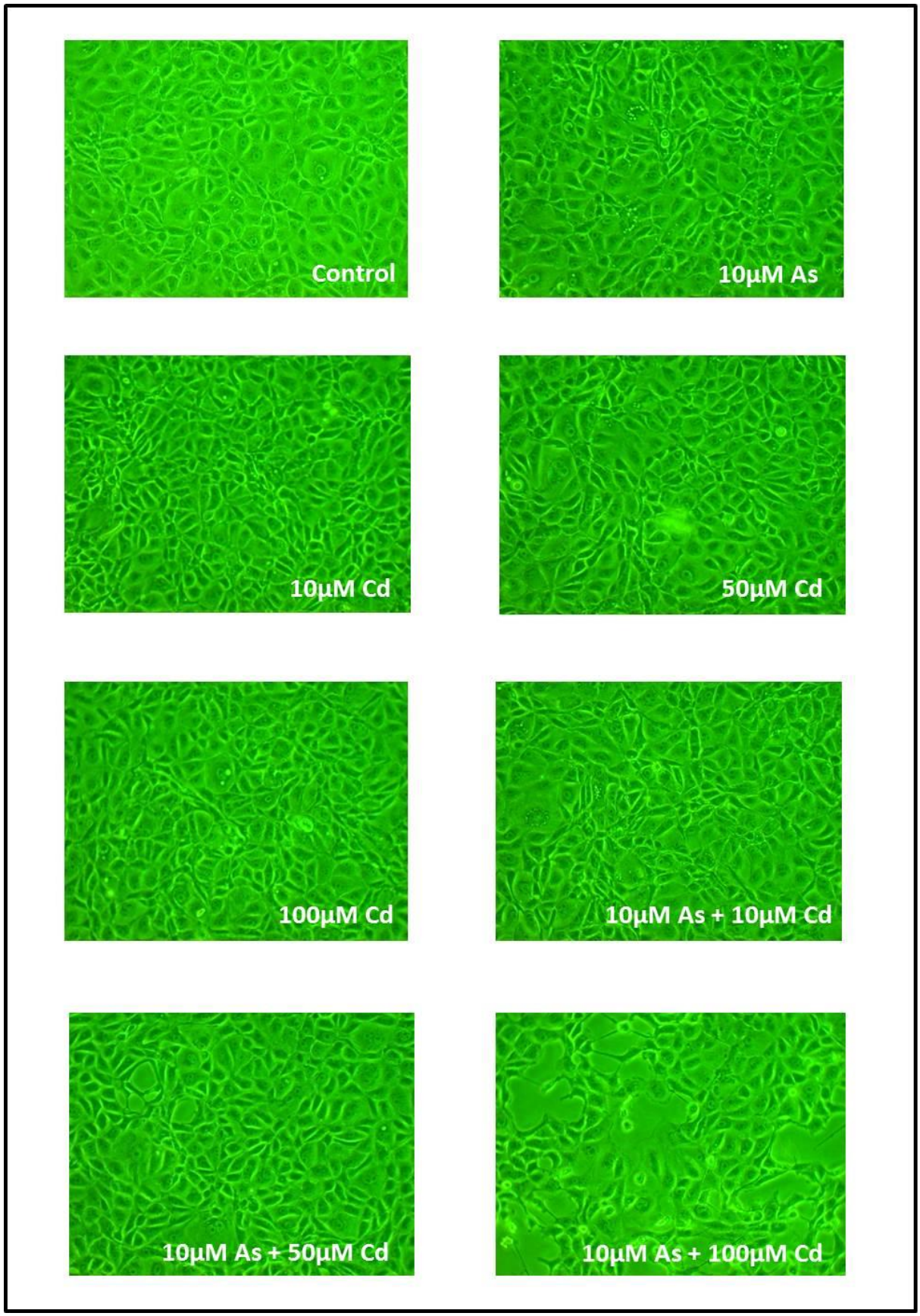
Control
10µM As
10µM Cd
50µM Cd
100µM Cd
10µM As + 10µM Cd
10µM As + 50µM Cd
10µM As + 100µM Cd

Figure 11. Time course of HSP30 and HSP70 accumulation in A6 cells treated simultaneously with low concentrations of sodium arsenite and cadmium chloride. A6 cells were maintained at 22 °C for 24 h (C), or incubated with 10 μM sodium arsenite (As) plus either 10 μM (panel A), 50 μM (panel B) or 100 μM (panel C) cadmium chloride (Cd) from 4 to 24 h at 22 °C. Immunoblot analysis of isolated total protein to detect the relative levels of HSP30, HSP70 and actin was performed as detailed in Materials and methods. These results are representative of 2 different experiments.

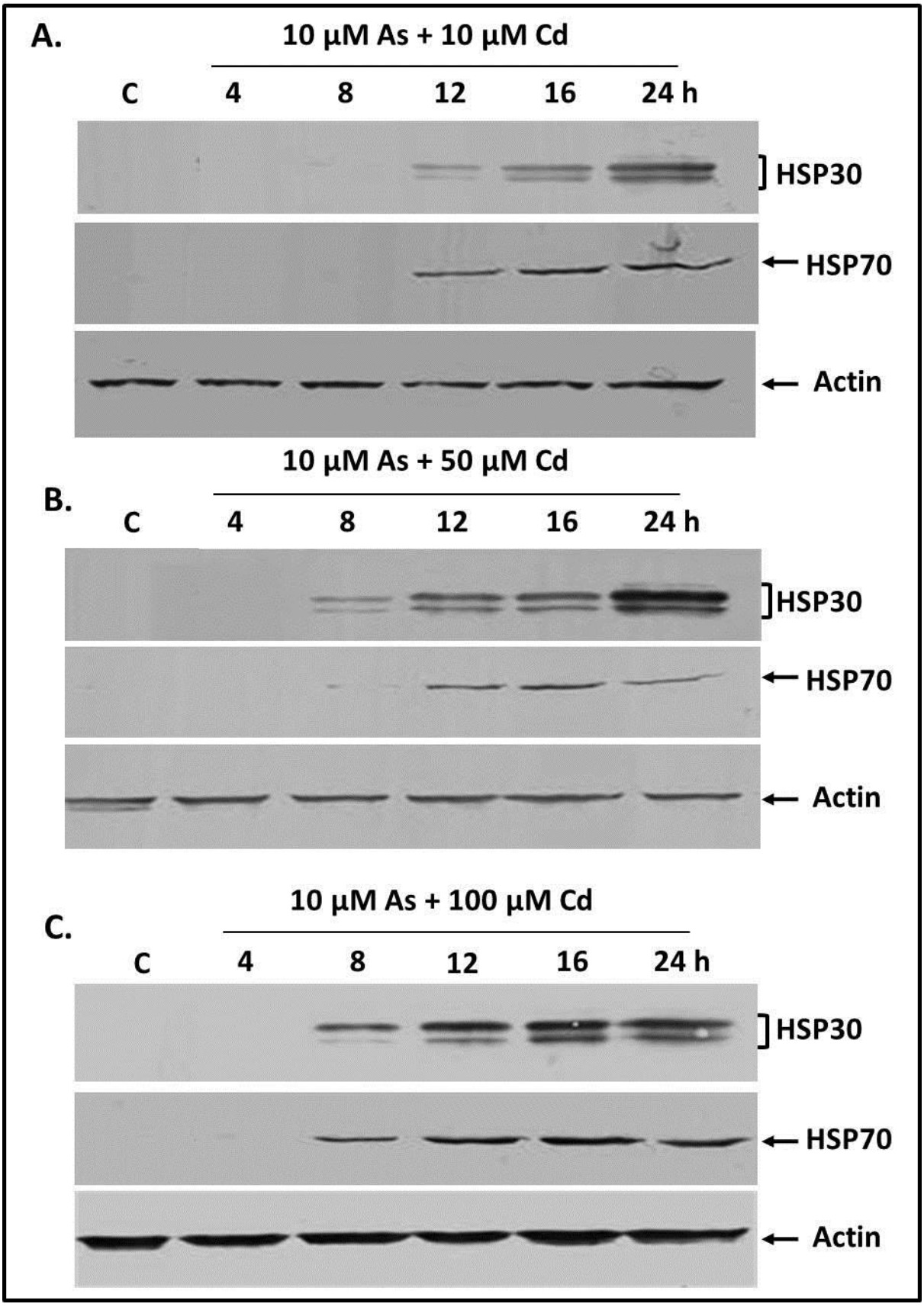
A.
10 µM As + 10 µM Cd
C
4
8
12
16
24 h
HSP30
HSP70
Actin
B.
10 µM As + 50 µM Cd
C
4
8
12
16
24 h
HSP30
HSP70
Actin
C.
10 µM As + 100 µM Cd
C
4
8
12
16
24 h
HSP30
HSP70
Actin

Figure 12. Extended time course of HSP30 and HSP70 accumulation in A6 cells treated simultaneously with low concentrations of sodium arsenite and cadmium chloride. A6 cells were maintained at 22 °C for 48 h (C) or incubated with 10 μM sodium arsenite (As) plus either 10 μM, 50 μM or 100 μM cadmium chloride (Cd) for 16, 24 or 48 h at 22 °C. Immunoblot analysis of isolated total protein was performed to detect the relative levels of HSP30, HSP70 and actin as detailed in Materials and methods. These results are representative of 2 different experiments.

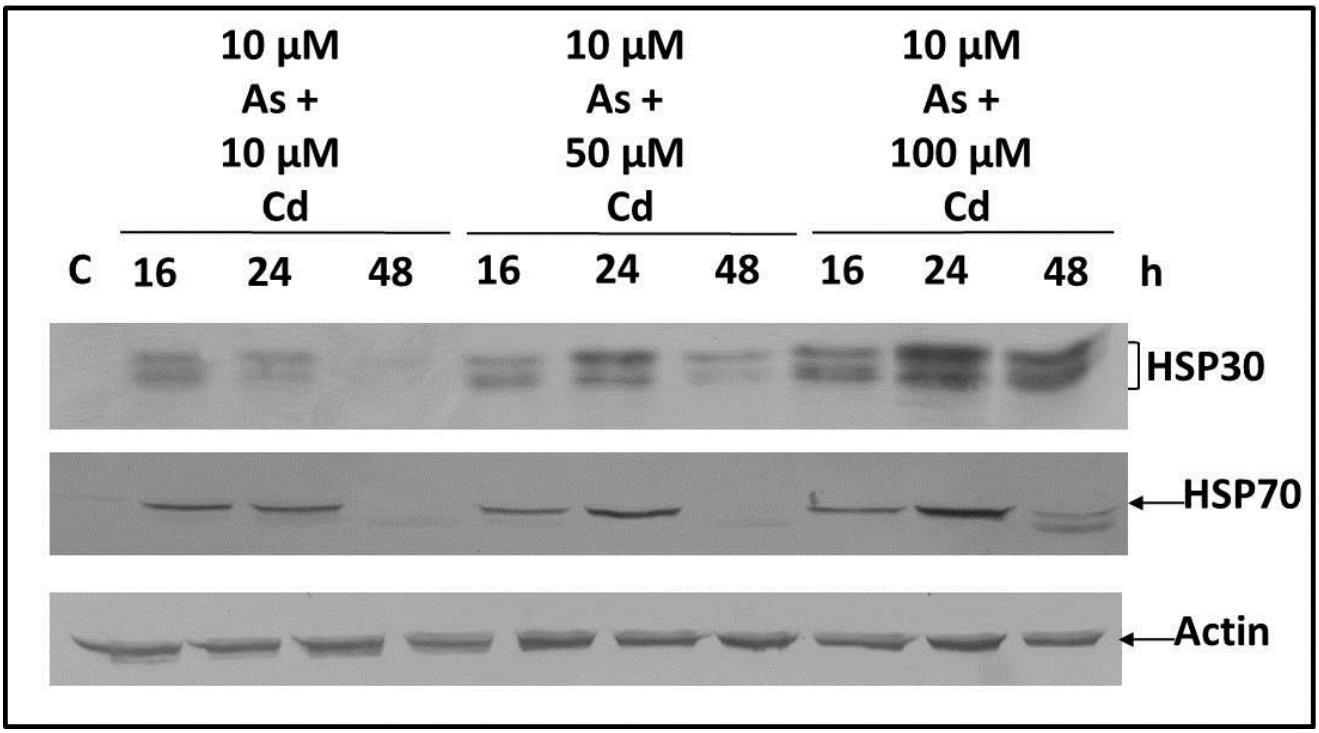
10 µM
As +
10 µM
Cd
10 µM
As +
50 µM
Cd
10 µM
As +
100 µM
Cd
C
16
24
48
16
24
48
16
24
48
h
HSP30
HSP70
Actin

Figure 13. Effect of either 2.5 or 5 μM sodium arsenite plus 50 μM cadmium chloride on HSP30 and HSP70 accumulation. A) A6 cells were maintained at 22 °C (C) or incubated with 50 μM cadmium chloride (Cd) and/or 2.5 or 5 μM sodium arsenite (As) for 12 h. Total protein was isolated and HSP30, HSP70 and actin was detected by immunoblot analysis as described in Materials and methods. B) Densitometric analysis of HSP30 (white bars) and HSP70 (black bars) was performed as described in Materials and methods and the results are expressed as a percentage of the maximum hybridization signal obtained for each protein (5 μM sodium arsenite plus 50 μM cadmium chloride for HSP30 and HSP70). Error bars represent standard error. Significant differences compared to control are indicated as * ($p < 0.05$). These results are representative of 3 different experiments.

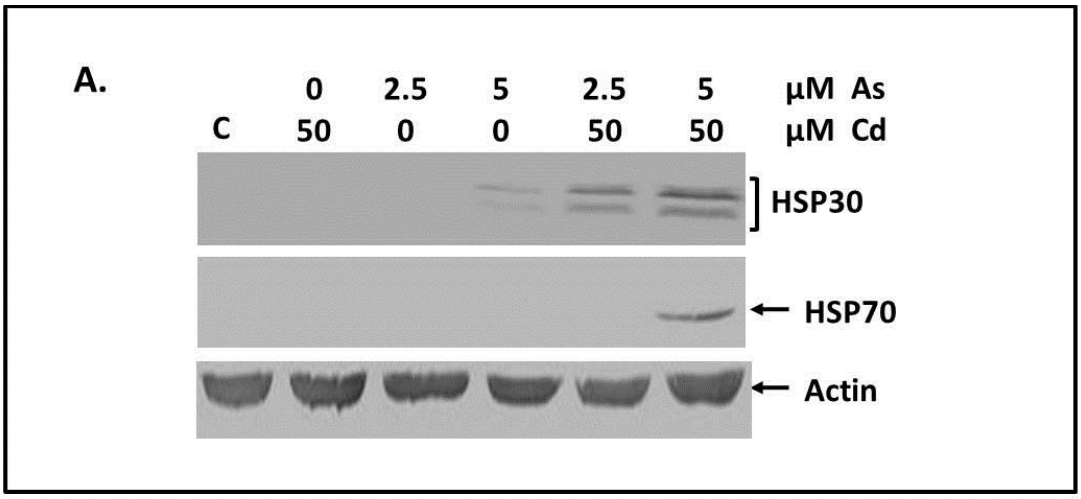
A.
C
0
50
2.5
0
5
0
2.5
50
5
50
µM As
µM Cd
HSP30
HSP70
Actin

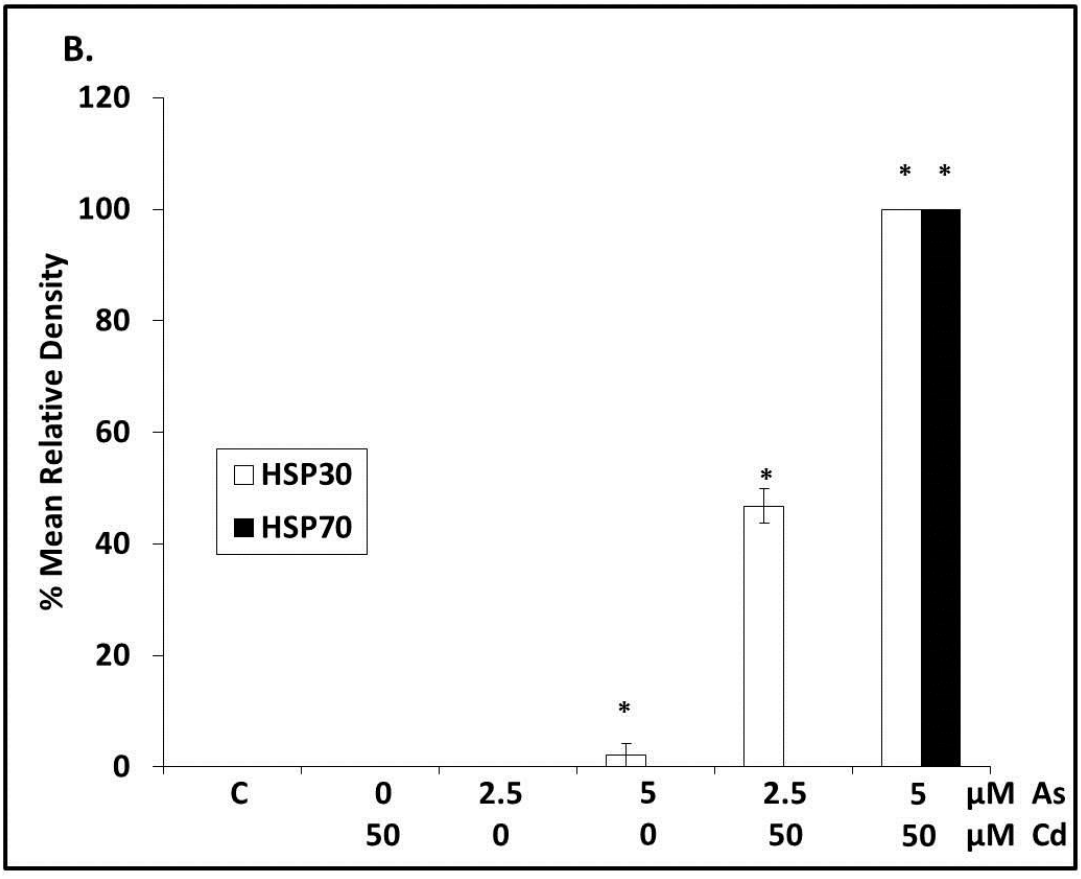
B.
% Mean Relative Density
120
100
80
60
40
20
0
HSP30
HSP70
*
*
*
*
C
0
50
2.5
0
5
0
2.5
50
5
50
µM As
µM Cd

Finally, cells that were treated simultaneously with sodium arsenite and cadmium chloride (at the concentrations employed in this study), and then allowed to recover in fresh media continued to undergo cell division and displayed a control-like appearance for at least 5 days, which was the end point of the recovery experiment (data not shown).

3.4 Effect of KNK437 on HSP30 and HSP70 accumulation in cells exposed simultaneously to sodium arsenite and cadmium chloride treatment

Previous studies in our laboratory and others determined that heat shock or chemical stress-induced accumulation of HSPs in *Xenopus laevis* was controlled, at least in part, at the transcriptional level by the activation of HSF1 (Ovsenek and Heikkila, 1990; Gordon et al., 1997; Heikkila, 2004; Manwell and Heikkila, 2007; Voyer and Heikkila, 2008). In the present study, I employed 100 μM KNK437 pretreatment to determine if the enhanced accumulation of HSP30 and HSP70 resulting from the concurrent sodium arsenite and cadmium chloride treatment involved HSF1 activation. This concentration of KNK437 was found to suppress *hsp* gene expression by inhibiting HSF1-HSE binding activity in a variety of eukaryotic model systems including human, mouse and *Xenopus* cultured cells with no detectable effect on viability of cells (Ohnishi et al., 2004; Manwell and Heikkila, 2007; Voyer and Heikkila, 2008; Young et al., 2009; Young and Heikkila, 2010; Brunt et al., 2012). Pretreatment of A6 cells with KNK437 suppressed the accumulation of HSP30 and HSP70 induced by simultaneous exposure to 10 μM sodium arsenite plus 50 or 100 μM cadmium chloride for 16 h by 90-100%, as shown in Figure 14. The levels of actin remained relatively constant throughout the experiment.

Figure 14. Effect of KNK437 on the accumulation of HSP30 and HSP70 in A6 cells treated concurrently with sodium arsenite and cadmium chloride. A) Cells were maintained at 22 °C or treated with 10 μM sodium arsenite (As) plus either 50 or 100 μM cadmium chloride for 16 h. Additionally, some cells were pretreated with 100 μM KNK437 for 6 h at 22 °C prior to the aforementioned treatments. Total protein was isolated and subjected to immunoblot analysis. B) Densitometric analysis of HSP30 (white bars) and HSP70 (black bars) was performed as described in Materials and methods. In each set of KNK437 treatments the values obtained in the presence of KNK437 were expressed as a percentage of the values obtained in its absence. Error bars indicate standard error. Significant differences between cells pretreated with or without KNK437 are indicated as * ($p < 0.05$). These results are representative of 5 different experiments.

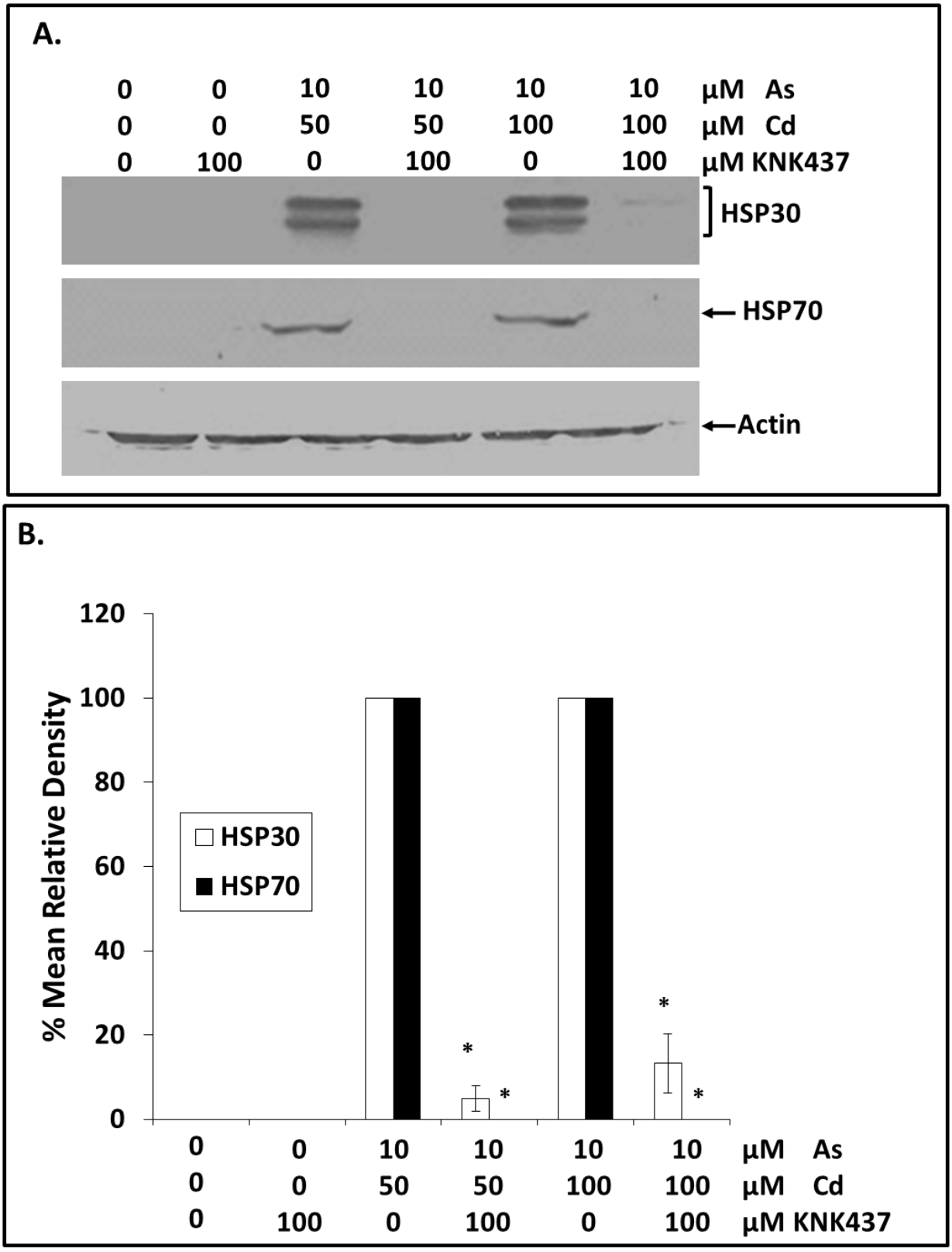
A.
0 0 10 10 10 10 µM As
0 0 50 50 100 100 µM Cd
0 100 0 100 0 100 µM KNK437
HSP30
HSP70
Actin
B.
% Mean Relative Density
120
100
80
60
40
20
0
HSP30
HSP70
*
0 0 10 10 10 10 µM As
0 0 50 50 100 100 µM Cd
0 100 0 100 0 100 µM KNK437

3.5 HSP30 localization in cells treated concurrently with sodium arsenite and cadmium chloride

The localization of HSP30 was determined by means of immunocytochemistry and laser scanning focal microscopy (LSCM). HSP70 localization was not carried out since the affinity-purified polyclonal anti-HSP70 antibody, which was successfully employed in immunoblot detection, was unable to specifically detect HSP70 by immunocytochemistry (Gauley et al., 2008). HSP30 accumulation was not detectable in control or cells treated with 10 μM cadmium chloride, but was qualitatively observed with 10 μM sodium arsenite in approximately 60% of the cells, indicated in Figure 15. In contrast, cells treated simultaneously with 10 μM cadmium chloride plus 10 μM sodium arsenite displayed strong HSP30 accumulation in 75% of the cells. Treatment of cells with 50 μM cadmium chloride, as shown in Figure 16, resulted in an accumulation of HSP30 in only 10% of the cells. However, when cells were exposed concurrently with 10 μM sodium arsenite and 50 μM cadmium chloride, 90% of the cells had a strong accumulation of HSP30. When this experiment was repeated with 10 μM sodium arsenite plus 100 μM cadmium chloride in Figure 17, the number of cells showing HSP30 was 95%. HSP30 accumulation was consistently detected in a granular pattern primarily in the cytoplasm with stronger staining near the periphery of some cells. An examination of the stressor treated cells stained for F-actin revealed the presence of membrane ruffling (white arrows) of the F-actin cytoskeleton. This membrane ruffling was more pronounced in cells treated simultaneously with combined stressor treatments than with the individual stressors alone.

Figure 15. Detection of HSP30 accumulation in A6 cells exposed to 10 μM sodium arsenite and/or 10 μM cadmium chloride. Cells were cultured on glass coverslips in L-15 media for 12 h at 22 °C in the absence (control) or presence of either 10 μM sodium arsenite (As), 10 μM cadmium chloride (Cd) or 10 μM sodium arsenite plus 10 μM cadmium chloride. Actin and nuclei were stained directly with phalloidin conjugated to TRITC (red) and with DAPI (blue), respectively. HSP30 was detected indirectly by an anti-HSP30 antibody and Alexa-488 secondary antibody conjugate (green). From left to right the columns display the fluorescence channels for actin, HSP30 and merged images plus DAPI. These results are representative of 3 different experiments.

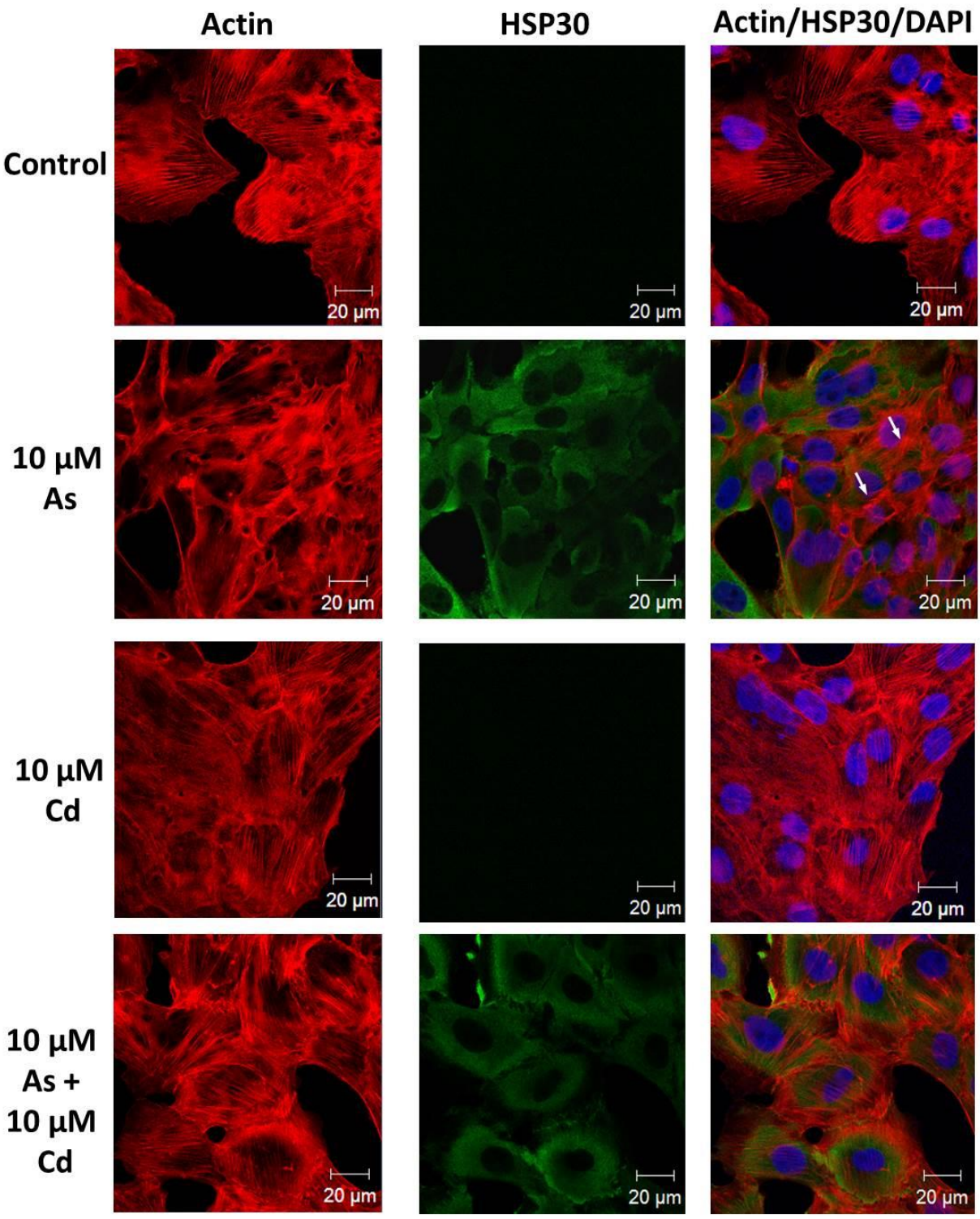
Actin
HSP30
Actin/HSP30/DAPI
Control
10 µM As
10 µM Cd
10 µM As + 10 µM Cd
20 µm

Figure 16. Detection of HSP30 accumulation in A6 cells exposed to 10 μM sodium arsenite and/or 50 μM cadmium chloride. Cells were cultured on glass coverslips in L-15 media for 12 h at 22 °C in the absence (control) or presence of either 10 μM sodium arsenite (As), 50 μM cadmium chloride (Cd) or 10 μM sodium arsenite plus 50 μM cadmium chloride. Actin and nuclei were stained directly with phalloidin conjugated to TRITC (red) and with DAPI (blue), respectively. HSP30 was detected indirectly by an anti-HSP30 antibody and Alexa-488 secondary antibody conjugate (green). From left to right the columns display the fluorescence channels for actin, HSP30 and merged images plus DAPI. These results are representative of 3 different experiments.

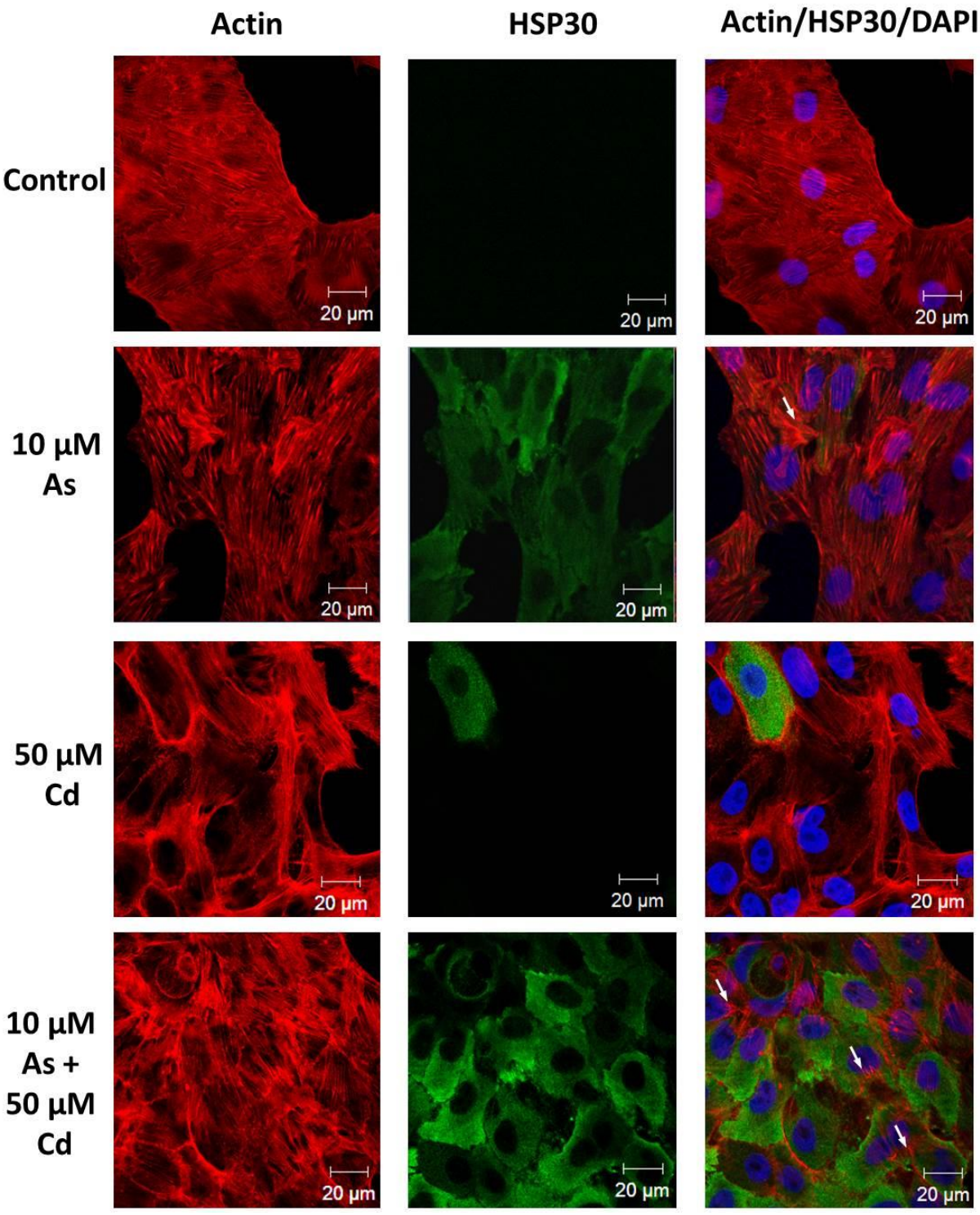
Actin
HSP30
Actin/HSP30/DAPI
Control
10 µM As
50 µM Cd
10 µM As + 50 µM Cd
20 µm

Figure 17. Detection of HSP30 accumulation in A6 cells exposed to 10 μM sodium arsenite and/or 100 μM cadmium chloride. Cells were cultured on glass coverslips in L-15 media for 12 h at 22 °C in the absence (control) or presence of either 10 μM sodium arsenite (As), 100 μM cadmium chloride (Cd) or 10 μM sodium arsenite plus 100 μM cadmium chloride. Actin and nuclei were stained directly with phalloidin conjugated to TRITC (red) and with DAPI (blue), respectively. HSP30 was detected indirectly by an anti-HSP30 antibody and Alexa-488 secondary antibody conjugate (green). From left to right the columns display the fluorescence channels for actin, HSP30 and merged images plus DAPI. These results are representative of 3 different experiments.

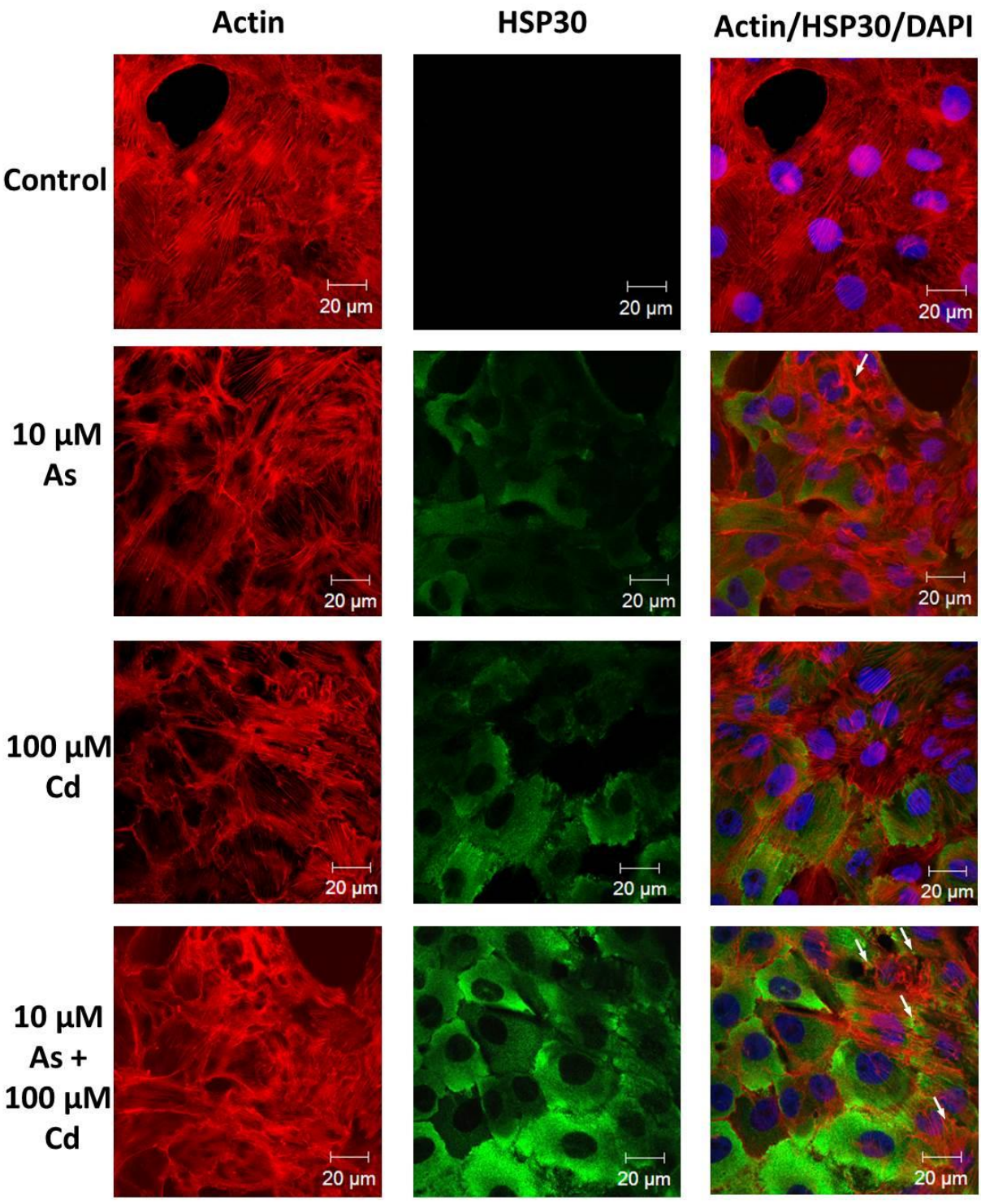
Actin
HSP30
Actin/HSP30/DAPI
Control
10 µM As
100 µM Cd
10 µM As + 100 µM Cd
20 µm

3.6 Effect of simultaneous sodium arsenite and cadmium chloride treatment on ubiquitinated protein levels

Inhibition of the proteasome in A6 cells by proteasomal inhibitors such as MG132 or lactacystin was reported to elevate the relative levels of ubiquitinated protein as found in other systems (Malik et al., 2001; Lehman, 2009; Young and Heikkila, 2010). Additionally, treatment of A6 cells individually with either sodium arsenite or cadmium chloride also induced an elevation in the ubiquitinated protein (Brunt et al., 2012). Given these findings, a comparison was made between the effect of individual and combined stressor treatments on the levels of ubiquitinated protein, as shown in Figure 18. Treatment of cells with 30 μM MG132, a reversible proteasomal inhibitor, induced a strong accumulation of ubiquitinated protein. In contrast, exposure of cells to 50 μM cadmium chloride displayed a ubiquitinated protein pattern similar to control whereas 100 μM cadmium chloride or 10 μM sodium arsenite produced a slight increase in ubiquitinated protein relative to control. Interestingly, the simultaneous exposure of cells to 10 μM sodium arsenite plus 50 or 100 μM cadmium chloride for 16 h enhanced the accumulation of ubiquitinated protein compared to the different stressors individually.

3.7 Effect of a concurrent mild heat shock plus low concentrations of sodium arsenite and cadmium chloride on HSP30, HSP70 and ubiquitinated protein accumulation

Finally, I examined the effect of combining a mild continuous 30 ºC heat shock with concurrent sodium arsenite and cadmium chloride treatment on HSP30, HSP70 and ubiquitinated protein accumulation (Fig. 19 and 20). In order to ensure visualization of the possible effect of an added mild thermal stress, lower concentrations of sodium arsenite and cadmium chloride were employed. Detectable levels of HSP30 and HSP70 were only observed when 1 μM sodium

Figure 18. Effect of combined sodium arsenite and cadmium chloride treatment on ubiquitinated protein accumulation in A6 cells. Cells were maintained at 22 °C in the absence or presence of sodium arsenite (As; 10 µM) or cadmium chloride (Cd; 50 or 100 µM) either individually or in combination at 22 °C. Some cells were treated with 30 µM MG132, a proteasomal inhibitor. All treatment times were 16 h. Immunoblot analysis of isolated total protein to detect the relative levels of ubiquitinated protein and actin was performed as detailed in Materials and methods. These results are representative of 2 different experiments.

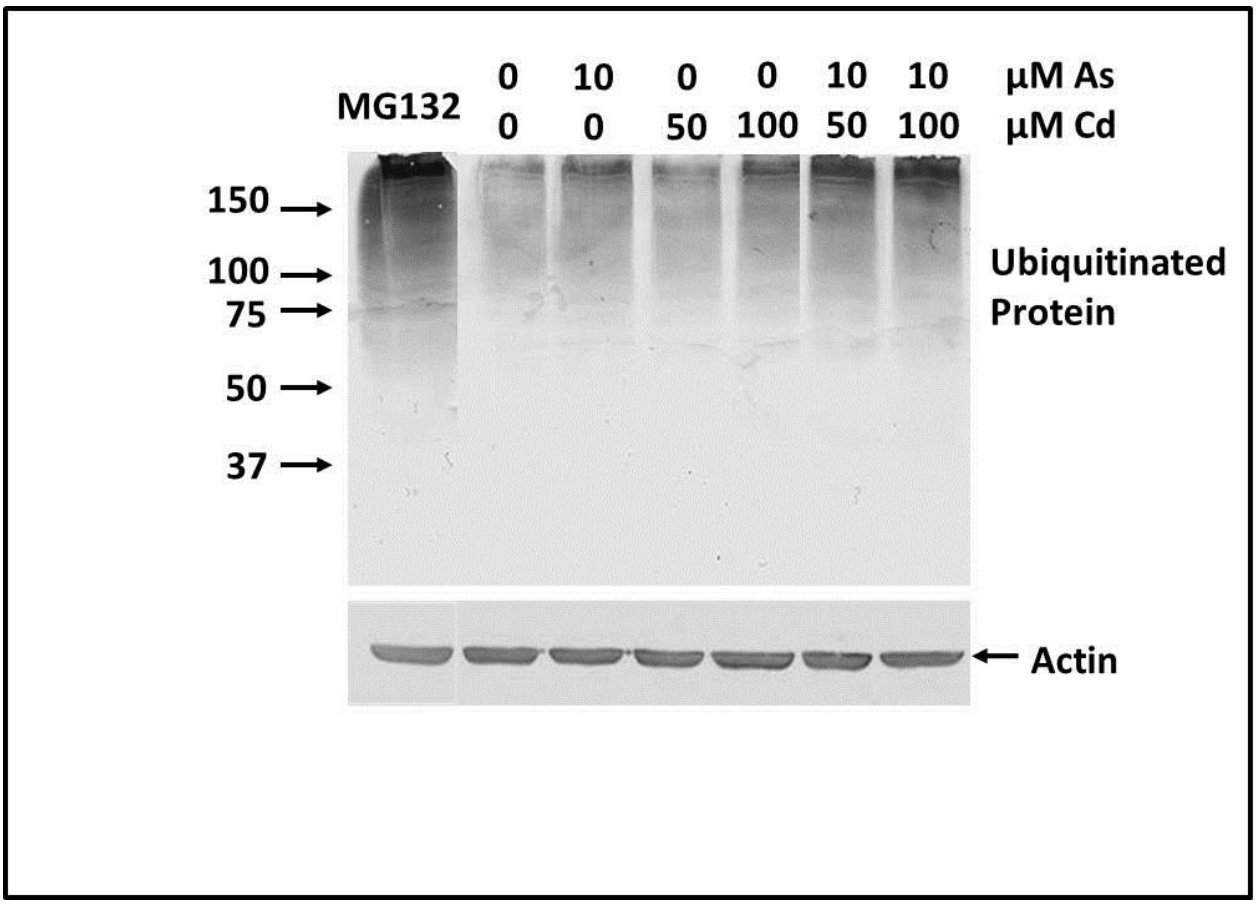
MG132
0 10 0 0 10 10 µM As
0 0 50 100 50 100 µM Cd
150
100
75
50
37
Ubiquitinated Protein
Actin

Figure 19. Accumulation of HSP30 and HSP70 in A6 cells treated simultaneously with relatively low concentrations of sodium arsenite, cadmium chloride plus a mild heat shock. A) Cells were treated with either 1 μM sodium arsenite (As) and/or 10 μM cadmium chloride (Cd) at 22 °C for 12 h or treated simultaneously with 1 μM sodium arsenite and/or 10 μM cadmium chloride at 30 °C for 12 h. Some flasks were maintained at 22 °C or 30 °C for 12 h. Total protein was isolated and subjected to immunoblot analysis to detect the relative levels of HSP30, HSP70 and actin as detailed in Materials and methods. B) Densitometric analysis of HSP30 (white bars) and HSP70 (black bars) from 3 different experiments was performed as detailed in Materials and methods. Results are expressed as a percentage of the maximum signal obtained for each protein (simultaneous treatment of cells with 1 μM sodium arsenite plus 10 μM cadmium chloride at 30 °C for both HSP30 and HSP70). Error bars represent the standard error. Significant differences compared to control are indicated as * ($p < 0.05$).

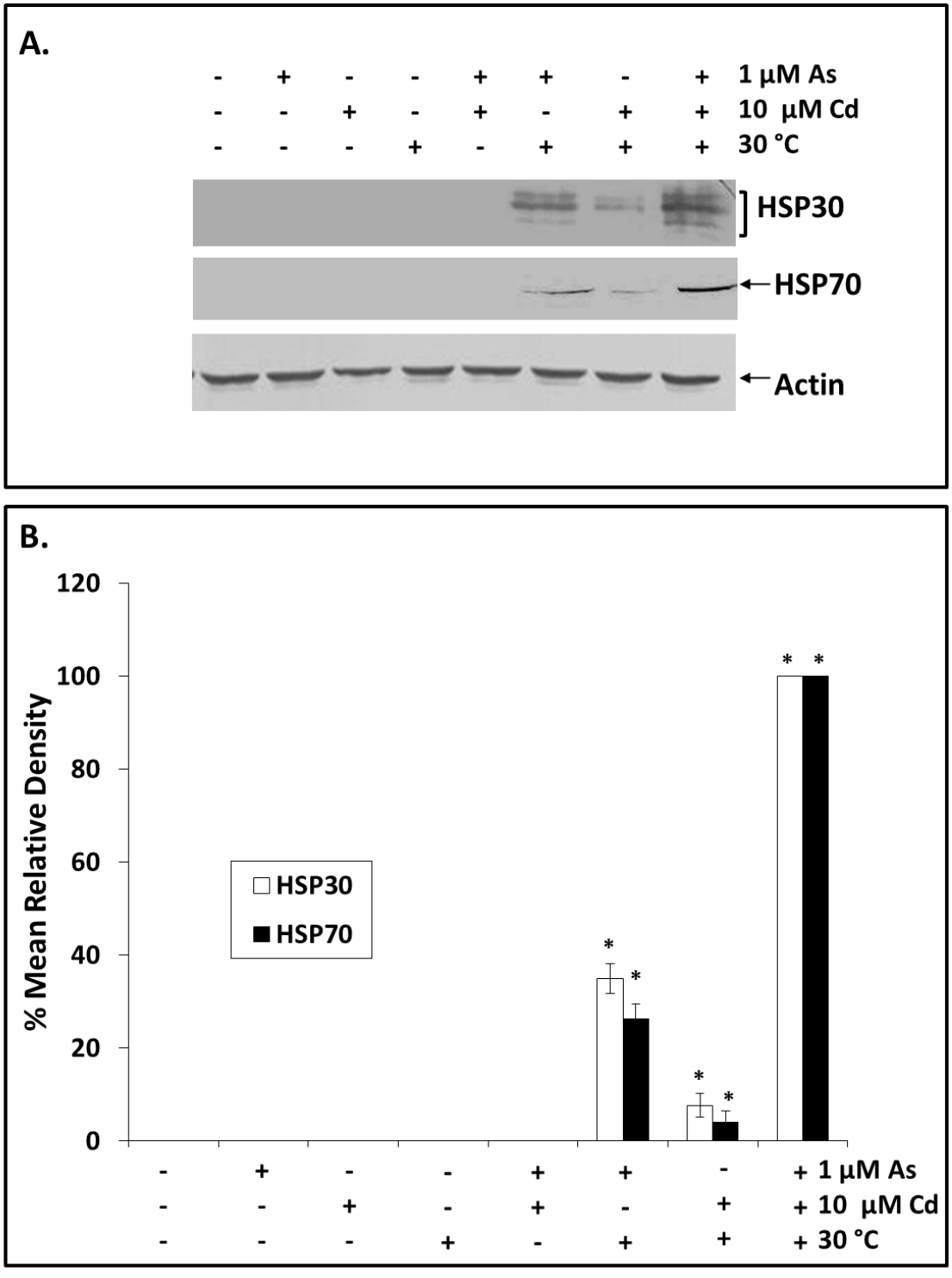
A.
- + - - + + - + 1 µM As
- - + - + - + + 10 µM Cd
- - - + - + + + 30 °C
HSP30
HSP70
Actin
B.
% Mean Relative Density
120
100
80
60
40
20
0
HSP30
HSP70
- + - - + + - + 1 µM As
- - + - + - + + 10 µM Cd
- - - + - + + + 30 °C

Figure 20. Effect of combined low concentrations of sodium arsenite and cadmium chloride plus mild heat shock treatment on ubiquitinated protein accumulation in A6 cells. Cells were maintained at 22 °C, or treated with 1 µM sodium arsenite (As) or 10 µM cadmium chloride (Cd), either individually or in combination at 22 °C or 30 °C for 12 h. Immunoblot analysis of isolated total protein to detect the relative levels of ubiquitinated protein and actin was performed as detailed in Materials and methods. These results are representative of 2 different experiments.

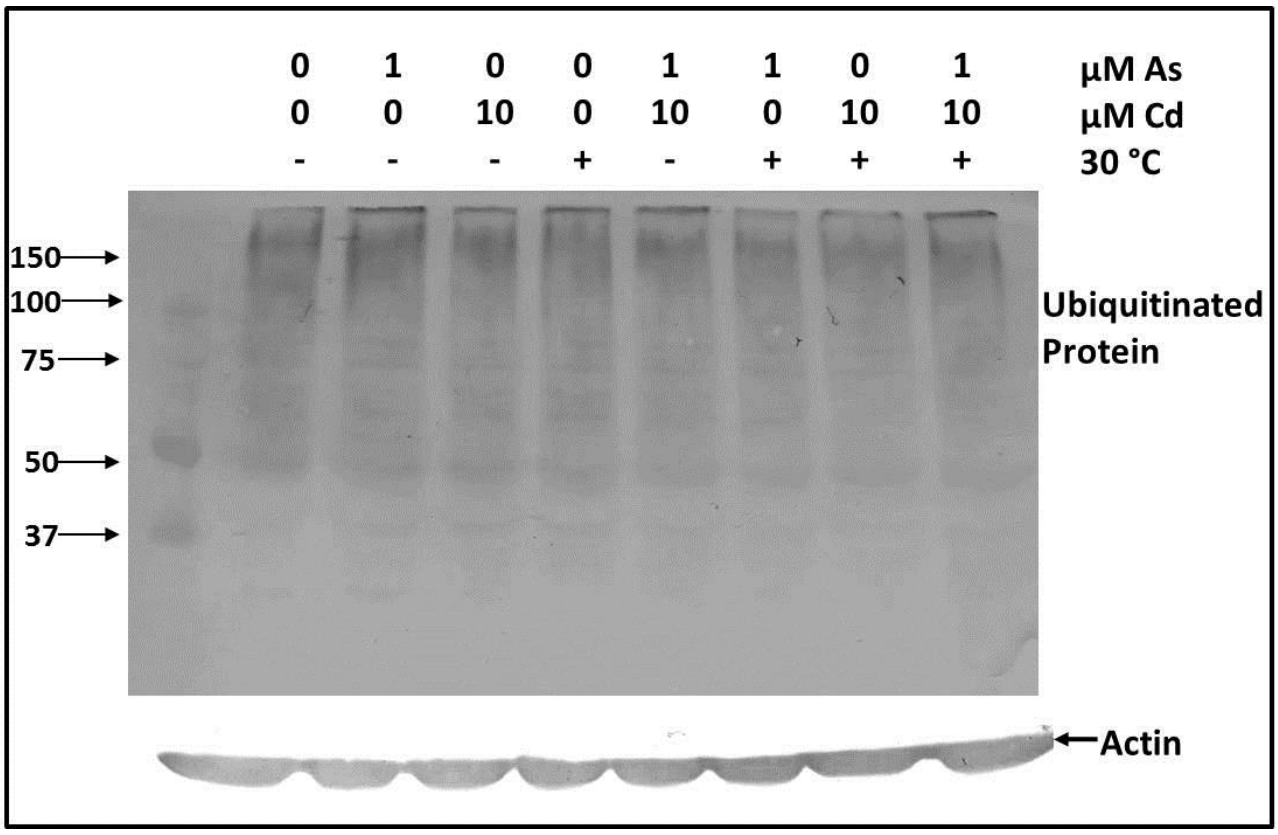
0 1 0 0 1 1 0 1 µM As
0 0 10 0 10 0 10 10 µM Cd
- - - + - + + + 30 °C
150
100
75
50
37
Ubiquitinated Protein
Actin

arsenite or 10 μM cadmium chloride treated cells were incubated at 30 °C, or all 3 stressors were employed together, as shown in Figure 20A. Denistometric analysis in Figure 19B confirmed that 1 μM sodium arsenite plus 30 ºC moderately enhanced the accumulation of both HSPs compared to a reduced accumulation of HSP30 and HSP70 observed with 10 μM cadmium chloride at 30 ºC. In comparison, the simultaneous treatment of cells with all 3 stressors greatly enhanced the accumulation of both HSP30 and HSP70. Pretreatment of cells with KNK437 inhibited the accumulation of HSP30 and HSP70 induced by all three stressors (data not shown).

The level of ubiquitinated protein accumulation, as shown in Figure 20, remained relatively constant between the 12 h treatments, as there was no significant increase observed in ubiquitinated protein with combining 2 stressors, or treatment with all 3 stressors together, compared to individual treatments. The relative levels of actin remained constant throughout these experiments.

4. Discussion

The present study has shown, for the first time in poikilotherms, that concurrent exposure of cells to relatively low concentrations of sodium arsenite plus cadmium chloride induced an enhanced accumulation of HSP30 and HSP70 in a dose-dependent fashion. Preliminary experiments involved the selection of the *Xenopus* A6 cell line to be used in these experiments. The magnitude of HSP30 accumulation was used as the key criteria since the anti-*Xenopus* HSP30 antibody detected this sHSP by both immunoblotting and immunocytochemistry. In contrast, the anti-*Xenopus* HSP70 antibody functioned quite well in immunoblots but did not specifically detect HSP70 by immunocytochemistry. Additionally, our laboratory has accumulated a great deal of information with respect to HSP30 accumulation in A6 cells. *Xenopus* A6 cells were chosen over XTC-2 cells since A6 cells demonstrated a stronger accumulation of HSP30 than XTC-2 cells in response to 20, 30 and 50 µM sodium arsenite treatments.

A second set of preliminary studies explored the use of various heavy metals at different concentrations to examine their effect on HSP30 accumulation in A6 cells. Treatment with zinc sulfate (100, 200, 300 or 500 µM), lead nitrate (5, 10, 25 or 50 µM) or copper sulfate (100, 200, 300, 500 or 1000 µM) for 8 h had either no detectable effect or induced a relatively low level of HSP30. In contrast, previous studies in our laboratory have shown treatment of A6 cells with either sodium arsenite or cadmium chloride produced an increase in HSP30 and HSP70 accumulation in a concentration-dependent manner. Furthermore, treatment of cells with these two metals simultaneously resulted in an enhanced accumulation of HSP30 and HSP70. The magnitude of these responses was greater than the sum of the individual stressors suggesting that sodium arsenite and cadmium chloride acted synergistically. Except for two preliminary studies

showing this phenomenon in mammalian tissue culture cells, there is a paucity of information on the effect of combined sodium arsenite and cadmium chloride treatment on HSP accumulation in animal systems (Madden et al., 2002; Eichler et al., 2005). Another example of the synergistic action of chemical stressors on *hsp* gene expression includes the potentiating effect of diethyl maleate or buthionine sulfoximine on either sodium arsenite or cadmium chloride-induced HSP27 accumulation in C6 rat glioma cells (Ito et al., 1998). Unfortunately, this latter study did not examine the combined effect of sodium arsenite and cadmium chloride. Additionally, it was found that low concentrations of iron and aluminum act synergistically on HSP27 accumulation in human neural cells (Alexandrov et al., 2005).

The mechanism for the synergistic action of sodium arsenite and cadmium chloride in the production of enhanced relative levels of HSP30 and HSP70 in *Xenopus* is unclear at present. However, the involvement of HSF1 activation was suggested since KNK437 pretreatment inhibited concurrent sodium arsenite and cadmium chloride-induced HSP30 and HSP70 accumulation. Previously, we demonstrated that KNK437 pretreatment of A6 cells inhibited HSP accumulation induced by sodium arsenite or cadmium chloride individually (Voyer and Heikkila, 2008; Woolfson and Heikkila, 2009). Also, Gordon et al. (1997) demonstrated that sodium arsenite and cadmium chloride induced the specific binding of HSF1 to HSE by gel shift assays. An accumulation of misfolded or non-native protein was indicated as being a trigger for HSF1 activation and thereby inducing *hsp* gene expression (Morimoto, 1998; Voellmy, 2004). It is known that arsenite can cause oxidative damage of proteins as well as attack sulfhydryl groups and thus impair protein function (Del Razo et al., 2001; Samuel et al., 2005). Furthermore, cadmium can react with vicinal thiol groups, cause oxidative protein damage and substitute for zinc in certain proteins (Waisberg et al., 2003; Galazyn-Sidorczuk et al., 2009). It is possible

that concurrent treatment of A6 cells with sodium arsenite and cadmium chloride produced an extensive range of protein damage resulting in an enhanced accumulation of misfolded protein compared to either stressor alone. This phenomenon could then trigger a strong activation of HSF1-HSE binding ultimately leading to an augmented accumulation of HSP30 and HSP70. This possible mechanism is illustrated in Figure 21.

Immunocytochemical analysis confirmed the enhanced accumulation of HSP30 in A6 cells treated simultaneously with sodium arsenite (10 μM) and cadmium chloride (10, 50 or 100 μM) compared to cells treated with these stressors individually. In cells treated with these mixtures, HSP30 accumulation occurred primarily in the cytoplasm in a granular pattern that likely reflects the formation of stress-induced multimeric structures, which appear to be necessary for their function in binding to unfolded cellular protein and inhibiting their aggregation (Ohan et al., 1998; MacRae, 2000; Fernando and Heikkila, 2000; Van Montfort, 2002; Fernando et al., 2003). An examination of F-actin cytoskeleton was performed since the architecture of the F-actin cytoskeleton has been employed as an indicator of cell health and viability (Ohtsuka et al., 1993; Wiegant et al., 1987). Treatment of A6 cells with the different concentrations of cadmium chloride displayed an F-actin cytoskeleton pattern that was similar to control. However, treatment of cells with 10 μM sodium arsenite alone or in combination with cadmium chloride produced F-actin cytoskeletal disorganization and membrane ruffling in some cells which were similar to that found with higher concentrations of either sodium arsenite or cadmium chloride as reported previously in A6 cells (Gellalchew and Heikkila, 2005; Woolfson and Heikkila, 2009). Cadmium chloride- and sodium arsenite-induced F-actin cytoskeletal disruptions including membrane ruffling were reported in mammalian cultured cells (Mills and Ferm, 1989; Li and Chou, 1992; Wang et al., 1996; Lii et al., 2010; Templeton and Liu, 2013).

Figure 21. Proposed mechanism of synergistic action of low concentrations of sodium arsenite plus cadmium chloride. Treatment of cells with relatively low concentrations of either chemical stressor individually results in the accumulation of unfolded protein within the cell that is not enough to activate HSF1. However, upon concurrent treatment of cells with sodium arsenite and cadmium chloride, the magnitude of intracellular unfolded protein increases to a threshold level that results in the sequestration of HSP90 by unfolded protein and the subsequent trimerization, hyperphosphorylation and binding of HSF1 to HSEs. This results in the expression of *hsp*30 and *hsp*70 genes leading to an accumulation of HSP30 and HSP70 to aid in the prevention of aggregation of unfolded protein.

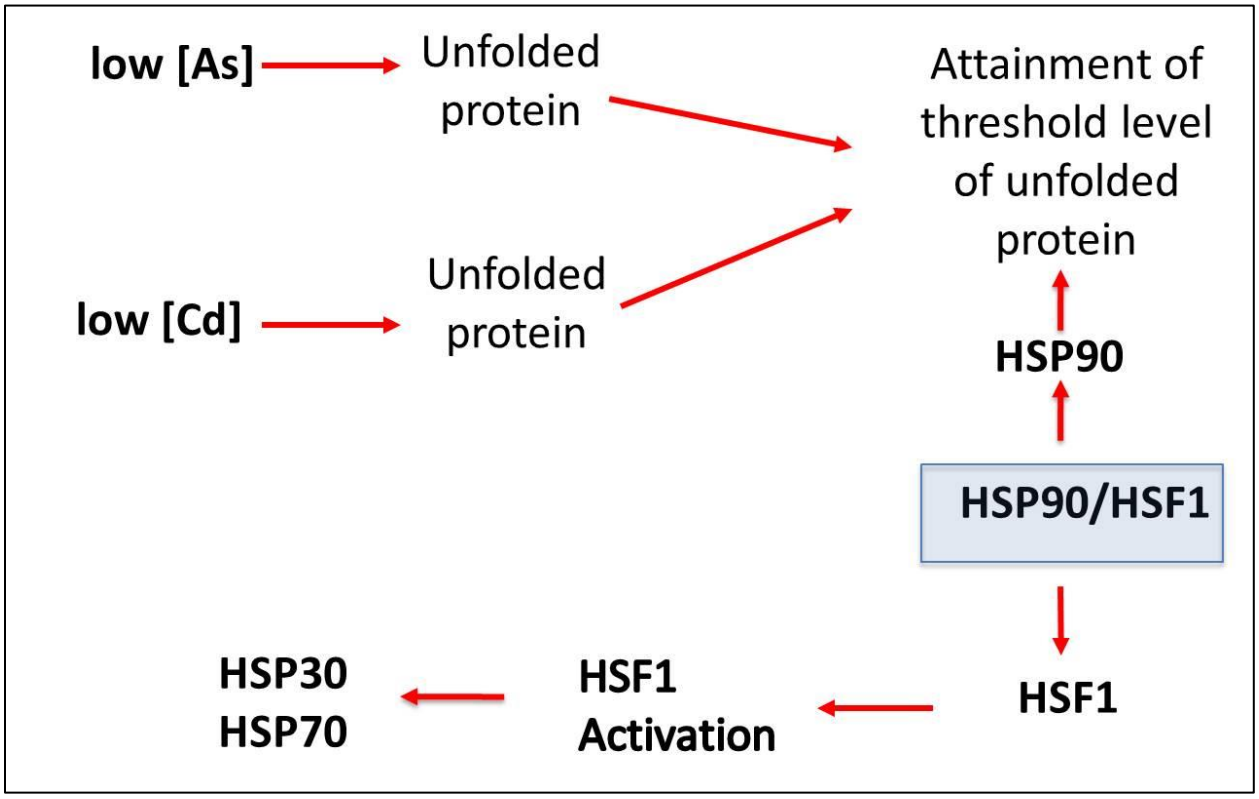
low [As]
Unfolded protein
low [Cd]
Unfolded protein
Attainment of threshold level of unfolded protein
HSP90
HSP90/HSF1
HSF1
HSF1 Activation
HSP30
HSP70

While the exact mechanisms are unknown, recent studies indicated that sodium arsenite caused the generation of carbonylated proteins that can lead to cytoskeletal damage, while cadmium-induced F-actin cytoskeletal damage may involve the actin-severing function of gelsolin, a key regulator of actin filament assembly and disassembly (Apostolova et al., 2006; Lii et al., 2010; Templeton and Liu, 2013).

In eukaryotic systems, the UPS is the primary degradation pathway for misfolded or damaged proteins (Lee and Goldberg, 1998). Previous studies have shown that inhibiting the activity of the proteasome leads to the accumulation of damaged or unfolded proteins within cells which are targeted for degradation by the addition of polyubiquitin chains (Bush et al., 1997; Lee and Goldberg, 1998; Malik et al., 2001; Liao et al., 2006). The present study determined that simultaneous treatment of A6 cells with relatively low concentrations of sodium arsenite and cadmium chloride enhanced the accumulation of ubiquitinated protein, an indicator of proteasomal inhibition. Previously, we reported that relatively higher concentrations of sodium arsenite (20 μM) or cadmium chloride (200 μM) than those used in this study were required to induce a strong accumulation of ubiquitinated protein (Brunt et al., 2012). It is possible that the simultaneous exposure of relatively low concentrations of sodium arsenite plus cadmium chloride may modify or damage key proteins associated with proteasome functioning. Furthermore, treatment of culture cells with sodium arsenite or cadmium chloride was reported to alter the normal expression of genes involved in protein ubiquitination and formation of proteasome subunits (Rea et al., 2003; Su et al., 2006; Yu et al., 2010).

In the present study, the addition of a concurrent mild heat shock of 30 ºC to A6 cells treated simultaneously with 1 μM sodium arsenite and 10 μM cadmium chloride potentiated the relative levels of HSP30 and HSP70. All three stressors appeared to act synergistically since the

magnitude of the HSP accumulation was greater than the sum of the responses obtained for the different stressors individually. While we are not aware of other studies reporting the synergistic action of a mild heat shock combined with a mixture of low concentrations sodium arsenite and cadmium chloride, previous studies in our laboratory did find that a mild heat shock plus a low concentration of either sodium arsenite or cadmium chloride acted synergistically in the induction of HSP30 and HSP70 in A6 cells (Young et al., 2009; Woolfson and Heikkila, 2009). Previous studies with mammalian and fish model systems demonstrated that the cellular uptake of arsenite and cadmium increased with elevated temperatures (McGeachy and Dixon, 1989; Souza et al., 1997; Saydam et al., 2003). Thus, it is possible that mild heat shock may increase the cellular uptake of cadmium chloride or sodium arsenite in A6 cells, which could increase the amount of denatured or misfolded protein and then activate the heat shock response. Given the potential lethality of a proteotoxic stress, it is essential to increase the relative levels of HSPs to counteract this threat.

While this study has provided some insight into the effects of simultaneous treatment with sodium arsenite and cadmium chloride on the heat shock response in A6 cells, future studies could explore the effect of these combined stressors on the acquisition of thermotolerance. Previous studies in our laboratory determined that prior exposure of A6 cells to a low concentration of sodium arsenite (10 μM) in combination with a mild heat shock (30 °C) conferred thermotolerance (Young et al., 2009). This meant that the cells were protected against a subsequent lethal thermal challenge at 37 °C. Therefore, future experiments could determine whether the synergistic action of concurrent sodium arsenite and cadmium chloride treatment in A6 cells could also confer thermotolerance.

Additional studies could also examine the effect of simultaneous sodium arsenite and cadmium chloride treatment on HSP accumulation in *Xenopus* embryos. Previous studies with embryos have determined the toxic and genotoxic potential of sodium arsenite or cadmium chloride alone. For instance, during *Xenopus* development, treatment of early embryos with sodium arsenite resulted in malformations and altered thyroid hormone-induced tail resorption during metamorphosis (Gornati et al., 2000; Davey et al., 2008). Furthermore, cadmium chloride exposure resulted in altered thyroid gland activity, ocular anomalies, bent notochord and heart, kidney, ovary and gut dysplasia (Sunderman et al., 1991; Plowman et al., 1994; Mouchet et al., 2006; Sharma and Patino, 2008). While the aforementioned studies investigated the detrimental toxic effects these chemical stressors on embryos individually, there is a lack of information available on the effect of combined sodium arsenite and cadmium chloride treatment on their toxicity and pattern of HSP accumulation.

References

Abdulle, R., Mohindra, A., Fernando, P., Heikkila, J.J. 2002. *Xenopus* small heat shock proteins, Hsp30C and Hsp30D, maintain heat- and chemically-denatured luciferase in a folding-competent state. Cell Stress Chaperones. 7, 6-16.

Adhikari, A., Sridhar K., Rangaraj, N., Parnaik, K., Mohan, C. 2004. Heat stress-induced localization of small heat shock proteins in mouse myoblasts: intranuclear lamin A/C speckles as target for alphaB-crystallin and Hsp25. Exp. Cell Res. 299, 393-403.

Alexandrov, P.N., Zhao, Y., Pogue, A.I., Tarr, M.A., Kruck, T.P.A., Percy M.E., Cui, J.E., Lukiw, W.J. 2005. Synergistic effects of iron and aluminum on stress-related gene expression in primary human neural cells. J. Alzheimer's Dis. 8, 117-127.

Ali, A., Krone, P., Heikkila, J.J. 1993. Expression of endogenous and microinjected hsp30 genes in early *Xenopus* tadpoles. Development 103, 59-67.

Ali, A., Salter-Cid, L., Flajnik, M.F., Heikkila, J.J. 1996a. Isolation and characterization of a cDNA encoding a *Xenopus* 70-kDa heat shock cognate protein, Hsc70.I. Comp. Biochem. Physiol. B. Biochem. Mol. Biol. 113,681-687.

Ali, A., Salter-Cid, L., Flajnik, M.J., Heikkila, J.J. 1996b. Molecular cloning of a cDNA encoding a *Xenopus* laevis 70-kDa heat shock cognate protein, hsc70.II. Biochem. Biophys. Acta. 1309, 174-178.

Ali, A., Fernando, P., Smith, W.L., Ovsenek, N., Lepock, J.R., Heikkila, J.J. 1997. Preferential activation of HSF-binding activity and *hsp*70 gene expression in *Xenopus* heart after mild hyperthermia. Cell Stress Chaperones. 2, 229-237.

Ali, A., Bharadwaj, S., O'Carroll, R., Ovsenek, N. 1998. Hsp 90 interacts with and regulates the activity of heat shock factor 1 in *Xenopus* oocytes. Mol Cell Biol. 18, 4949-4960.

Allen, S.P., Polazzi, J.O., Gierse, J.K., Easton, A.M. 1992. Two novel heat shock genes encoding proteins produced in response to heterologous protein expression in *Escherichia coli*. J. Bacteriol. 174, 6938-6947.

Apostolova, M.D., Christova, T., Templeton, D.M. 2006. Involvement of gelsolin in cadmium-induced disruption of the mesangial cell cytoskeleton. Toxicol. Sci. 89, 465-474.

Arrigo, A-P. 1998. Small stress proteins: chaperones that act as regulators of intracellular redox state and programmed cell death. Biol. Chem. 379, 19-26.

Arrigo, A-P., Landry, J. 1994. Expression and function of the low-molecular weight heat shock proteins. In: Morimoto R.I., Tissieres A., Georgopoulos, C. *The biology of heat shock*

proteins and molecular chaperones pp. 335-373. Cold Spring Harbor, New York: Cold Spring Harbor Laboratory Press.

Arriizumi, T., Sawamura, K., Uchiyama, H., Asashima, M. 1991. Dose and time-dependent mesoderm induction and outgrowth formation by activin A in *Xenopus laevis.* Int. J. Dev. Biol. 35, 407-414.

Balch, W.E., Morimoto, R.I., Dillin A., Kelly J.W. 2008. Adapting proteostasis for disease intervention. Science. 319, 916-919.

Beaulieu, J.F., Arrigo, A-P., Tanguay, R.M. 1989. Interaction of *Drosophila* 27,000 Mr heat-shock protein with the nucleus of heat-shocked and ecdysone-stimulated culture cells. J. Cell Sci. 92, 29-36.

Beckman, R.P., Mizzen, L.E., Welch, W.J. 1990. Interaction of Hsp 70 with newly synthesized proteins: implications for protein folding and assembly. Science. 248, 850-854.

Bedford, L., Paine, S., Sheppard, P.W., Mayer, R.J., Roelofs, J. 2010. Assembly, structure, function of the 26S proteasome. Trends Cell Biol. 20, 391-401.

Beere, H.M., Wolf, B.B., Cain, K., Mosser, D.D., Mahboubi, A., Kuwana, T., Tailor, P., Morimoto, R.I., Cohen, G.M., Green, D.R. 2000. Heat-shock protein 70 inhibits apoptosis by preventing recruitment of procaspase-9 to the apaf-1 apoptosome. Nat. Cell Biol. 2, 469-475.

Bienz, M. 1984. Developmental control of the heat shock response in *Xenopus*. Proc. Natl. Acad. Sci. USA. 81, 3138-3142.

Bogyo, M., Gaczynska, M., Ploegh, H.L. 1997. Proteasome inhibitors and antigen presentation. Biopolymers. 43, 269-280.

Bonham, R.T, Fine, M.R., Pollock, F.M., Shelden, E.A. 2003. Hsp27, Hsp70, and metallothionein in MDCK and LLC-PK1 renal epithelial cells: effects of prolonged exposure to cadmium. Toxicol. Appl. Pharmacol. 191, 63-73.

Boston, R.S., Viitanen, P.V., Vierling, E. 1996. Molecular chaperones and protein folding in plants. Plant Mol. Biol. 32, 191-222.

Briant, D., Ohan, N., Heikkila, J.J. 1997. Effect of herbimycin A on *hsp30* and *hsp70* heat shock protein gene expression in *Xenopus* cultured cells. Biochem. Cell Biol. 75, 777-782.

Brunt, J.J., Khan, S., Heikkila, J.J. 2012. Sodium arsenite and cadmium chloride induction of proteasomal inhibition and HSP accumulation in *Xenopus laevis* A6 kidney epithelial cells. Comp. Biochem. Physiol. C. Toxicol. Pharmacol. 155, 307-317.

Buchner, J., Ehrnsperger, M., Gaestel, M., Walke, S. 1998. Purification and characterization of small heat shock proteins. Methods Enzymol. 290, 339- 349.

Buckley, B.A., Owen, M.E., Hofmann, G.E. 2001. Adjusting the thermostat: the threshold induction temperature for the heat-shock response in intertidal mussels (genus *Mytilus*) changes as a function of thermal history. J. Exp. Biol. 204, 3571-3579.

Bush, K.T., Goldberg, A.L., Nigam, S.K. 1997. Proteasome inhibition leads to a heat-shock response, induction of endoplasmic reticulum chaperones, and thermotolerance. J. Biol. Chem. 272, 9086-9092.

Ciechanover, A., Heller, H., Elias, S., Haas, A.L., Hershko, A. 1980. ATP-dependent conjugation of reticulocyte proteins with the polypeptide required for protein degradation. Proc. Natl. Acad. Sci. USA. 77, 1365–1368.

Darasch, S., Mosser D.D., Bols, N.C., Heikkila, J.J. 1988. Heat shock gene expression in *Xenopus laevis* A6 cells in response to heat shock and sodium arsenite treatments. Biochem. Cell Biol. 66, 862-868.

Daugaard, M., Rohde, M., Jäättelä, M. 2007. The heat shock protein 70 family: Highly homologous proteins with overlapping and distinct functions. FEBS Lett. 581, 3702-3710.

Davey, J.C., Nomikos, A.P., Wungjiranirun, M., Sherman, J.R., Ingram, L., Batki, C., Lariviere, J.P., Hamilton, J.W. 2008. Arsenic as an endocrine disruptor: Arsenic disrupts retinoic acid receptor and thyroid hormone receptor-mediated gene regulation and thyroid hormone-mediated amphibian tail metamorphosis. Environ. Health Perspect. 116, 165-172.

Del Razo, L.M., Quintanilla-Vega, B., Brambila-Colombres, E., Calderon-Aranda, E.S., Manno M., Albores, A. 2001. Stress proteins induced by arsenic. Toxicol. Appl. Pharmacol. 177, 132-148.

Eichler, T.E., Ransom, R.F., Smoyer, W.E. 2005. Differential induction of podocyte heat shock proteins by prolonged single and combination toxic metal exposure. Toxicol. Sci. 84, 120-128.

Elicker, K.S., Huston, L.D. 2007. Genome-wide analysis and expression profiling of the small heat shock proteins in zebrafish. Gene. 403, 60-69.

Fernando, P., Megeney, L.A., Heikkila, J.J. 2003. Phosphorylation-dependent structural alterations in the small hsp30 chaperone are associated with cellular recovery. Exp. Cell Res. 286, 175-185.

Fort, D.J., Stover, E.L., Bantle, J.A., Dumont, J.N., Finch, R.A. 2001. Evaluation of reproductive toxicity assay using *Xenopus laevis*: boric acid, cadmium and ethylene glycol monomethyl ether. J. Appl. Toxicol. 21, 41-52.

Gaianaki, C., Pliatska, M., Stathopoulou, K., Beis, I. 2006. Cu^{2+} and acute thermal stress induce protective events *via* the p38-MAPK signalling pathway in the perfused *Rana ridibunda* heart. J. Exp. Biol. 210, 438-446.

Galazyn-Sidorczuk, M., Brzoska, M.M., Jurczuk, M., Moniuszko-Jakoniuk, J. 2009. Oxidative damage to proteins and DNA exposed to cadmium and/or ethanol. Chem. Biol. Interact. 180, 31-38.

Gauley, J., Young J.T., Heikkila, J.J. 2008. Intracellular localization of the heat shock protein, HSP110, in *Xenopus laevis* A6 kidney epithelial cells. Comp. Biochem. Physiol. A Mol. Integr. Physiol. 153, 417-424.

Gellalchew, M., Heikkila, J.J. 2005. Intracellular localization of *Xenopus* small heat shock protein, hsp30, in A6 kidney epithelial cells. Cell Biol. Int. 29, 221-227.

Georgopoulos, C., Welch, W.J. 1993. Role of the major heat shock proteins as molecular chaperones. Annu. Rev. Cell Biol. 9, 601-634.

Gordon, S., Bharadwaj, S., Hnatov, A., Ali, A., Ovsenek, N. 1997. Distinct stress-inducible and developmentally regulated heat shock transcription factors in *Xenopus* oocytes. Dev. Biol. 181, 47-63.

Gornati, R., Monetti, C., Vigetti, D., Bosisio, S., Fortaner, S., Sabbioni, E., Bernardini, G., Prati, M. 2002. Arsenic toxicity and HSP70 expression in *Xenopus laevis* embryos. Altern. Lab. Anim. 30, 597-603.

Gothard, L.Q., Ruffner, M.E., Woodward, J.G., Park-Sarge, O.K., Sarge, K.D. 2003. Lowered temperature set point for activation of the cellular stress response in T-lymphocytes. J. Biol. Chem. 278, 9322-9326.

Guerra, L., Favia, M., Fanelli, T., Calamita, G., Svetlo, M., Bagorda, A., Jacobson, K.A., Reshkin, S.J., Casavola, V. 2004. Stimulation of *Xenopus* P2Y1 receptor activates CFTR in A6 cells. Pflugers Arch. 449, 66-75.

Haslbeck, M. 2002. sHsps and their role in the chaperone network. Cell Mol. Life Sci. 59, 1649-1657.

Hatayama, T., Asai, Y., Wakatsuki, T., Kitamura, T., Imahara, H. 1993. Regulation of hsp70 Synthesis induced by Cupric Sulfate and Zinc Sulfate in Thermotolerant HeLa Cells. J. Biochem. 114, 592-597.

Heikkila, J.J., Ohan, N., Tam, Y., Ali, A. 1997. Stress protein gene expression in Amphibians. In: Koval, T.M., *Stress-inducible processes in higher eukaryotic cells* Chapter 6 pp. 137-164. Plenum Press, New York.

Heikkila, J.J. 2003. Expression and function of small heat shock protein genes during *Xenopus* development. Semin. Cell. Dev. Biol. 14, 259-266.

Heikkila, J.J. 2004. Regulation and function of small heat shock protein genes during amphibian development. J. Cell Biochem. 93, 672-680.

Heikkila, J.J. 2010. Heat Shock protein gene expression and function in amphibian model systems. Comp. Biochem. Physiol. A. Mol. Integr. Physiol. 156, 19-33.

Helbing, C., Gallimore, C., Atkinson, B.G. 1996. Characterization of a *Rana catesbeiana* HSP30 gene and its expression in the liver of this amphibian during both spontaneous and thyroid hormone-induced metamorphosis. Dev. Genet. 18, 223-233.

Hershko, A., Ciechanover, A., Heller, H., Haas, A.L., Rose, I.A. 1980. Proposed role of ATP in protein breakdown: conjugation of proteins with multiple chains of the polypeptide of ATP-dependent proteolysis. Proc. Natl. Acad. Sci. USA. 77, 1783–1786.

Hough, R., Pratt, G., Rechsteiner, M. 1987. Purification of two high molecular weight proteases from rabbit reticulocyte lysate. J. Biol. Chem. 262, 8303–8313.

Ikuzawa, M., Akiduki, S., Asashima, M. 2007. Gene expression profile of *Xenopus* A6 cells cultured under random positioning machine shows downregulation of ion transporter genes and inhibition of dome formation. Adv. Space Res. 40, 1694-1702.

Ito, H., Okamoto, K., Kato, K. 1998. Enhancement of expression of stress proteins by agents that lower the levels of glutathione in cells. Biochem. Biophys. Acta. 1397, 223-230.

Joseph, P., Muchnok, T.K., Klishis, M.L., Roberts, J.R., Antonini, J.M., Whong, W.Z., Ong, T. 2001. Cadmium-induced cell transformation and tumourigenesis are associated with transcriptional activation of *c-fos*, *c-jun*, and *c-myc* proto-oncogenes: role of cellular calcium and reactive oxygen species. Toxicol. Sci. 61, 295-303.

Karn, H., Ovsenek, N., Heikkila, J.J. 1992. Examination of the DNAsequence-specific binding properties of heat shock transcription factor in *Xenopus laevis* embryos. Biochem. Cell Biol. 70, 1006-1013.

Katoh,Y., Fujimoto, M., Nakamura, K., Inouye, S., Sugahara, K., Izu, H., Nakai, A. 2004. Hsp25, a member of the Hsp30 family, promotes inclusion formation in response to stress. FEBS Lett. 565, 28-32.

Katschinski, D.M. 2004. On heat and cells and proteins. News Physiol. Sci. 19, 11-15.

Khan, S., Heikkila, J.J. 2011. Curcumin-induced inhibition of proteasomal activity, enhanced HSP accumulation and the acquisition of thermotolerance in *Xenopus laevis* A6 cells. Comp. Biochem. Physiol. A Mol. Integr. Physiol. 158, 566-576.

Khan, S., Rammeloo, A., Heikkila, J.J. 2012. Withaferin A Induces Proteasome Inhibition, Endoplasmic Reticulum Stress, the Heat Shock Response and Acquisition of Thermotolerance. PLoS One. doi: 10.1371/journal.pone.0050547.

Kim, Y.K., Jang, S.K. 2002. Continuous heat shock enhances translational initiation directed by internal ribosomal entry site. Biochem. Biophys. Res. Commun. 297, 224-231.

Kirkpatrick, D.S., Dale, K.V., Catania, J.M., Gandolfi, A.J. 2003. Low-level arsenite causes accumulation of ubiquitinated proteins in rabbit renal cortical slices and HEK293 cells. Toxicol. Appl. Pharmacol. 186, 101-109.

Koegl, M., Hoppe, T., Schlenker S., Ulrich, H.D, Mayer, T.U, Jentsch, S. 1999. A novel ubiquitination factor, E4, is involved in multiubiquitin chain assembly. Cell. 96, 635-644.

Krebs, R.A., Feder, M.E. 1997. Tissue-specific variation in Hsp70 expression and thermal damage in *Drosophila melanogaster* larvae. J. Exp. Biol. 200, 2007-2015.

Kregel, K.C. 2002. Heat shock proteins: modifying factors in physiological stress responses and acquired thermotolerance. J. Appl. Physiol. 92, 2177-2186.

Krone, P.H., Snow, A., Ali, A., Pasternak, J.J., Heikkila, J.J. 1992. Comparison of the regulatory and structural regions of the *Xenopus laevis* small heat shock protein encoding gene family. Gene. 110, 159-166.

Lambert, H., Charette, S.J., Bernier, A.F., Guimond, A., Landry, J. 1999. HSP27 multimerization mediated by phosphorylation-sensitive intermolecular interactions at the amino terminus. J. Biol. Chem. 274, 9378-9385.

Lang, L., Miskovic, D., Fernando, P., Heikkila, J.J. 1999. Spatial pattern of constitutive and heat shock-induced expression of the small heat shock protein gene family, Hsp30, in *Xenopus laevis* tailbud embryos. Dev. Genet. 25, 365-374.

Lee, D.H., Goldberg, A.L. 1998. Proteasome inhibitors: valuable new tools for cell biologists. Trends Cell Biol. 8, 397-403.

Lehman, N.L. 2009. The ubiquitin proteasome system in neuropathology. Acta Neuropathol. 118, 329-347.

Li, W., Chou, I.N. 1992. Effects of sodium arsenite on the cytoskeleton and cellular glutathione levels in cultured cells. Toxicol. Appl. Pharmacol. 114, 132-139.

Liang, P., Amons, R., Clegg, J.S., MacRae, T.H. 1997. Molecular characterization of a small heat shock/α-crystallin protein in encysted *Artemia* embryos. J. Biol. Chem. 272, 19051-19058.

Liao, W., Li, X., Mancini, M., Chan, L. 2006. Proteasome inhibition induces differential heat shock protein response but not unfolded protein response in HepG2 cells. J. Cell Biochem. 99, 1085-95.

Lii, C.K., Lin, A.H., Lee, S.L., Chen, H.W., Wang, T.S. 2010. Oxidative modifications of proteins by sodium arsenite in human umbilical vein endothelial cells. Environ. Toxicol. 26, 459-471.

Linder, B., Jin, Z., Freeman, J.H., Rubin, C.S. 1996. Molecular characterization of a novel, developmentally regulated small embryonic chaperone from *Caenorhabditis elegans*. J. Biol. Chem. 271, 30158-30166.

Liu, J., Kadiiska, M.B., Liu, Y., Lu, T., Qu, W., Waalkes, M.P. 2001. Stress-related gene expression in mice treated with inorganic arsenicals. Toxicol. Sci. 61, 314-320.

Liu, Y., Zheng, T., Zhao, S., Liu, H., Han, D., Zhen, Y., Xu, D., Wang, Y., Yang, H., Zhang, G., Wang, C., Wu, J., Ye, Y. 2012. Inhibition of heat shock protein response enhances PS-341 glioma cell death. Ann. Surg. Oncol. 19 Suppl 3, 421-429.

Loumbourdis, N.S. 2005. Hepatoxic and nephrotoxic effects of Cadmium in the frog *Rana ridibunda*. Arch. Toxicol. 79, 434-440.

Ma, H.P. 2011. Hydrogen peroxide stimulates the epithelial sodium channel through a phophatidylinositide 3-kinase-dependant pathway. J. Biol. Chem. 286, 32444-32453.

MacRae, T.H. 2000. Structure and function of small heat shock/α-crystallin proteins: Established concepts and emerging ideas. Cell Mol. Life Sci. 57, 899-913.

Madden, E.F., Akkerman, M., Fowler, B.A. 2002. A comparison of 60, 70, and 90 kDa stress protein expression in normal rat NRK-52 and human HK-2 kidney cell lines following in vitro exposure to arsenite and cadmium alone or in combination. J. Biochem. Molec. Toxicol. 16, 24-32.

Malik, B., Schlanger, L., Al-Khalili, O., Bao, H.F., Yue, G., Price, S.R., Mitch, W.E., Eaton, D.C. 2001. Enac degradation in A6 cells by the ubiquitin-proteosome proteolytic pathway. J. Biol. Chem. 276, 12903-12910.

Manwell, L.A., Heikkila, J.J. 2007. Examination of KNK437- and quercetin-mediated inhibition of heat shock-induced heat shock gene expression in *Xenopus laevis* cultured cells. Comp. Biochem. Physiol. 148, 521-530.

Masliah, E., Rockenstein, E., Veinbergs, I., Mallory, M., Hashimoto, M., Takeda, A., Sagara, Y., Sisk, A., Mucke, L. 2000. Dopaminergic loss and inclusion body formation in alpha-synuclein mice: Implications for neurodegenerative disorders. Science. 287, 1265-1269.

McGeachy, S.M., Dixon, D.G. 1989. The impact of temperature on the acute toxicity of arsenate and arsenite to rainbow trout (*Salmo gairdneri*). Ecotoxicol. Environ. Saf. 17, 86-93.

Mendez-Armenta, M., Rios, C. 2007. Cadmium neurotoxicity. Environ. Toxicol. Pharmacol. 23, 350-358.

Michaud, S., Marin, R., Tanguay, R.M. 1997. Regulation of heat shock gene induction and expression during *Drosophila* development. Cell. Mol. Life Sci. 53, 104-113.

Mills, J.W., Ferm, V.H. 1989. Effect of cadmium on F-actin and microtubules of *Madin-Darby* canine kidney cells. Toxicol. Appl. Pharmacol. 101, 245-254.

Miskovic, D., Salter-Cid, L., Ohan, N., Flajnik, M., Heikkila, J.J. 1997. Isolation and characterization of a cDNA encoding a *Xenopus* immunoglobulin binding protein, BiP (grp78). Comp. Biochem. Physiol. B. Biochem. Mol. Biol. 116, 227-34.

Morimoto, R.I. 1998. Regulation of the heat shock transcriptional response: Cross talk between a family of heat shock factors, molecular chaperones, and negative regulators. Genes Dev. 12, 3788-3796.

Morimoto, R.I. 2008. Proteotoxic stress and inducible chaperone networks in neurodegenerative disease and aging. Genes Dev. 22, 1427-1438.

Morimoto, R.I., Santoro, M.G. 1998. Stress-inducible responses and heat shock proteins: New pharmacologic targets for cytoprotection. Nat. Biotechnol. 16, 833- 838.

Muller, M., Gauley, J., Heikkila, J.J. 2004. Hydrogen peroxide induces heat shock protein and proto-oncogene mRNA accumulation in *Xenopus laevis* A6 kidney epithelial cells. Can. J. Physiol. Pharmacol. 82, 523-529.

Murata, M., Gong, P., Suzuki, K., Koizumi, S. 1999. Differential metal response and regulation of human heavy metal-inducible genes. J Cell Physiol. 180, 105-113.

Nakai, A., Tanabe, M., Kawazoe, Y., Inazawa, J., Morimoto, R.I., Nagata, K. 1997. HSF4, a new member of the human heat shock factor family which lacks properties of a transcriptional activator. Mol Cell Biol. 17, 469-481.

Nissato, N., Ohta, M., Eaton, D.C., Marunaka, Y. 2012. Hypotonic stress upregulates β- and γ-ENaC expression through suppression of ERK by inducing MPK-1. Am. J. Physiol. Renal Physiol. 303, 240-252.

Norris, C.E., dilorio, P.J., Schultz, R.J., Hightower, L.E. 1995. Variation in heat shock proteins within tropical and desert species of Poeciliid fishes. Mol. Biol. Evol. 12, 1048-1062.

Ohan, N.W., Tam, Y., Fernando, P., Heikkila, J.J. 1998. Characterization of a novel group of basic small heat shock proteins in *Xenopus laevis* A6 kidney epithelial cells. Biochem. Cell Biol. 76, 665-671.

Ohnishi, K., Takahashi, A., Yokota, S., Ohnishi, T. 2004. Effects of a heat shock protein inhibitor KNK437 on heat sensitivity and heat tolerance in human squamous cell carcinoma cell lines differing in p53 status. Intl. J. Rad. Biol. 80, 607-614.

Ohtsuka, K., Liu, Y.C., Kaneda, T. 1993. Cytoskeletal thermotolerance in NRK cells. Int. J. Hyperthermia 9, 115-124.

Ovakim, D.H., Heikkila, J.J. 2003. Effect of histone deacetylase inhibitors on heat shock protein gene expression during *Xenopus* development. Genesis. 36, 88-96.

Ovsenek, N., Heikkila, J.J. 1990. DNA sequence-specific binding activity of the heat shock transcription factor is heat-inducible before midblastula transition of early *Xenopus* development. Development. 110, 427-433.

Pastoret, A., Marcos, R., Sampaya-Reyes, A., Saucedo-Cardenas, O., Lozano-Garza, G.H., Hernandez, A. 2012. Inhibition of hepatocyte nuclear factor 1 and 4 alpha (HNF1α and HNF4α) as a mechanism of arsenic carcinogens. Arch. Toxicol. 87, 1001-1012.

Pedersen, T.V., Bjerregaard, P. 2000. Cadmium influx and efflux across perfused gills of the shore crab, *Carcinus maenas.* Aquat. Toxicol. 48, 223-231.

Plowman, M.C., Grbac-Ivankovic, S., Martin, J., Hopfer, S.M., Sunderman, F.W. Jr. 1994. Malformations persist after metamorphosis of *Xenopus laevis* tadoles exposed to NI2+, Co2+, or Cd2+ in FETAX assays. Teratog. Carcinog. Mutagen. 14, 135-144.

Pudney, M., Varma, M.G.R., Leake, C.J. 1973. Establishment of a cell line (XTC-2) from the South African clawed toad, *Xenopus laevis*. Experientia. 29, 466-467.

Rafferty, K.A. 1969. Mass culture of amphibian cells: Methods and observations concerning stability of cell type. In: Mizell, M., *Biology of amphibian tumors* pp. 58-81. Berlin: Springer Verlag.

Rallu, M., Loones, M., Lallemand, Y., Morimoto, R., Morange, M., Mezger, V. 1997. Function and regulation of heat shock factor 2 during mouse embryogenesis. Proc. Natl. Acad. Sci. USA. 94, 2392-2397.

Rea, M.A., Gregg, J.P., Quin, Q., Phillips, M.A., Rice, R.H. 2003. Global alteration of gene expression human keratinocytes by inorganic arsenic. Carcinogenesis 24, 747-756.

Ritossa, F. 1962. A new puffing pattern induced by heat shock and DNP in *Drosophila*. Experimentia. 571-573.

Ross, C.A., Pickart, C.M. 2004. The ubiquitin–proteasome pathway in Parkinson's disease and other neurodegenerative diseases. Trends Cell Biol. 14, 703-711.

Samuel, S., Kathirvel, R., Jayavelu, T., Chinnakkannu, P. 2005. Protein oxidative damage in arsenic induced rat brain: influence of DL-alpha-lipoic acid. Toxicol. Lett. 155, 27-34.

Sarge, K.D. 1995. Male germ cell-specific alteration in temperature set point of the cellular stress response. J. Biol. Chem. 270, 18745-18748.

Saydam, N., Steiner, F., Georgiev, O., Schaffner, W. 2003. Heat and heavy metal stress synergize to mediate transcriptional hyperactivation by metal-responsive transcription factor MTF-1. J. Biol. Chem. 278, 31879-31883.

Schlesinger, M.J. 1990. Heat shock proteins. J. Biol. Chem. 265, 1211-12114.

Shamovsky, I., Nudler, E. 2008. New insights into the mechanism of heat shock response activation. Cell. Mol. Life Sci. 65, 855-861.

Sharma, B., Patino, R. 2008. Exposure of *Xenopus laevis* tadpoles to cadmium reveals concentration-dependent bimodal effects on growth and monotonic effects on development and thyroid gland activity. Toxicol. Sci. 105, 51-58.

Song, X., Chen, Z., Wu, C., Zhao, S. 2010. Abrogating HSP response augments cell death induced by As2O3 in glioma cell lines. Can. J. Neurol. Sci. 37, 504-511.

Souza, V., Bucio, L., Gutierrez-Ruiz, M.C. 2003. Cadmium uptake by a human hepatic cell line (WRL-68 cells). Toxicol. 120, 215-220.

Spicer, E., Suckert, C., Al-Attar, H., Marsden, M. Integrin alpha5beta1 function is regulated by XGIPC/kermit2 mediated endocytosis during *Xenopus laevis* gastrulation. PLos One. doi: 0.1371/journal.pone.0010665.

Stromer, T., Ehrnsperger, M., Gaestel, M., Buchner, J. 2003. Analysis of the interaction of small heat shock proteins with unfolding proteins. J. Biol. Chem. 278, 18015-18021.

Stumpf, H., Senkel, S., Rabes, H.M., Ryffel, G.U. 1995. The DNA binding activity of the liver transcription factors LFB1 (HNF1) and HNF4 varies coordinately in rat hepatocellular carcinoma. Carcinogenesis. 16, 143-145.

Su, P-F., Hu, Y-J., Ho, I-C., Cheng, Y-M., Lee, T.C. 2006. Distinct gene expression profiles in immortalized human urothelial cells exposed to inorganic arsenite and its methylated trivalent metabolites. Environ. Health Perspect. 114, 394-403.

Sun, Y., MacRae, T.H. 2005. The small heat shock proteins and their role in human disease. FEBS J. 272, 2613-2627.

Sunderman, F.W. Jr., Plowman, M.C., Hopfer, S.M. 1991. Embryotoxicity and teratogenicity of cadmium chloride in *Xenopus laevis*, assayed by the FETAX procedure. Ann. Clin. Lab. Sci. 21, 381-391.

Tai, H.C., Schuman, E.M. 2008. Ubiquitin, the proteasome and protein degradation in neuronal function and dysfunction. Nat. Rev. Neurosci. 9, 826-838.

Tam, Y., Heikkila, J.J. 1995. Identification of members of the HSP30 small heat shock protein family and characterization of their developmental regulation in heat-shocked *Xenopus laevis* embryos. Devel. Genet. 17, 331-339.

Templeton, D.M., Liu, Y. 2013. Effects of cadmium on the actin cytoskelton in renal mesangial cells. Can. J. Physiol. Pharacol. 91, 1-7.

Tsou, T.C., Tsai, F.Y., Hseih, Y.W., Li, L.A., Yeh, S.C., Chang, L.W. 2005. Arsenite induces endothelial cytotoxicity by down-regulation of vascular endothelial nitric oxide synthase. Toxicol. Appl. Pharmacol. 208, 277-284.

Van den Eijnden-Van Raaij, A.J., van Zoelent, E.J., van Nimmen, K., Koster, C.H., Snoek, G.T., Durston, A.J., Huylebroeck, D. 1990. Activin-like factor from a *Xenopus laevis* cell line responsible for mesoderm induction. Nature. 345, 732-734.

Van Montfort, R., Slingsby, C., Vierling, E. 2001. Structure and function of the small heat shock protein/alpha-crystallin family of molecular chaperones. Adv. Protein Chem. 59, 105-156.

Voellmy, R. 2004. On mechanisms that control heat shock transcription factor activity in metazoan cells. Cell Stress Chaperones. 9, 122-133.

Voyer, J., Heikkila, J.J. 2008. Comparison of the effect of heat shock inhibitor, KNK437 on heat shock- and chemical stress-induced hsp30 gene expression in *Xenopus laevis* A6 cells. Comp. Biochem. Physiol. A. Mol. Integr. Physiol. 151, 253-261.

Waisberg, M., Pius, J., Hale, B., Beyersmann, D. 2003. Molecular and cellular mechanisms of cadmium carcinogenesis. Toxicology. 192, 95-117.

Walcott, S.E., Heikkila, J.J. 2010. Celastrol can inhibit proteasome activity and upregulate the expression of heat shock protein genes, *hsp*30 and *hsp*70, in *Xenopus laevis* A6 cells. Comp. Biochem. Physiol. A. Mol. Integr. Physiol. 156, 285-293.

Wang, Z., Chin, T.A., Templeton, D.M. 1996. Calcium-independent effects of cadmium on actin assembly in mesangial and vascular smooth muscle cells. Cell Motil. Cytoskeleton. 33, 208-222.

Waters, E.R., Lee, G.J., Vierling, E. 1996. Evolution, structure and function of the small heat shock proteins in plants. J. Exp. Bot. 47, 325-338.

Wiegant, F.A., van Bergen en Henegouwen, P.M., van Dongen, G., Linnemans, W.A. 1987. Stress-induced thermotolerance of the cytoskeleton of mouse neuroblastoma N2A cells and rat *Reuber* H35 hepatoma cells. Cancer Res. 47, 1674-1680.

Wilkinson, K.D., Urban, M.K., Haas, A.L. 1980. Ubiquitin is the ATP-dependent proteolysis factor I of rabbit reticulocytes. J. Biol. Chem. 255, 7529–7532.

Woolfson, J.P., Heikkila, J.J. 2009. Examination of cadmium-induced expression of the small heat shock protein gene, hsp30 in *Xenopus laevis* A6 kidney epithelial cells. Comp. Biochem. Physiol. A. 152, 91-99.

Wotton, D., Freeman, K., Shore, D. 1996. Multimerization of Hsp42p, a novel heat shock protein of *Saccharomyces cerevisiae*, is dependent on a conserved carboxyl-terminal sequence. J. Biol. Chem. 271, 2717-2723.

Yamamoto, N., Takemori, Y., Sakurai, M., Sugiyama, K., Sakurai, H. 2009. Differential recognition of heat shock elements by members of the heat shock transcription factor family. FEBS J. 276, 1962-1974.

Yang, H., Landis-Piwowar, K.R., Chen, D., Milacic, V., Dou, Q.P. 2008. Natural compounds with proteasome inhibitory activity for cancer prevention and treatment. Curr. Protein Pept. Sci. 9, 227-239.

Young, J.T., Heikkila, J.J. 2009. Simultaneous exposure of *Xenopus* A6 kidney epithelial cells to concurrent mild sodium arsenite and heat stress results in enhanced hsp30 and hsp70 gene expression and the acquisition of thermotolerance. Comp. Biochem. Physiol. A. Mol. Int. Physiol. 153, 417-424.

Young, J.T., Heikkila, J.J. 2010. Proteasome inhibition induces *hsp30* and *hsp70* gene expression as well as the acquisition of thermotolerance in *Xenopus laevis* A6 cells. Cell Stress Chaperones 15, 323-334.

Yu, X., Hong, S., Faustman, E.M. 2008. Cadmium-induced activation of stress signaling pathways, disruption of ubiquitin-dependent protein degradation and apoptosis in primary rat sertoli cell-gonocyte cocultures. Toxicol. Sci. 104, 385-396.

Yu, X., Robinson, J.F., Sidhu, J.S., Hong, S., Faustman, E.M. 2010. A system-based comparison of gene expression reveals alterations in oxidative stress, disruption of ubiquitin-proteasome system and altered cell cycle regulation after exposure to cadmium and methylmercury in mouse embryonic fibroblast. Toxicol. Sci. 114, 356-377.

Zimmermann, R., Müller, L., Wullich, B. 2006. Protein transport into the endoplasmic reticulum: Mechanisms and pathologies. Trends Mol. Med. 12, 567-573.